Biol Cybern (2006) 95: 1–19
DOI 10.1007/s00422-006-0068-6

REVIEW

Biological Cybernetics

A. N. Burkitt

A review of the integrate-and-fire neuron model: I. Homogeneous synaptic input

Received: 2 August 2005 / Accepted: 20 March 2006 / Published online: 19 April 2006

Abstract The integrate-and-fire neuron model is one of the most widely used models for analyzing the behavior of neural systems. It describes the membrane potential of a neuron in terms of the synaptic inputs and the injected current that it receives. An action potential (spike) is generated when the membrane potential reaches a threshold, but the actual changes associated with the membrane voltage and conductances driving the action potential do not form part of the model. The synaptic inputs to the neuron are considered to be stochastic and are described as a temporally homogeneous Poisson process. Methods and results for both current synapses and conductance synapses are examined in the diffusion approximation, where the individual contributions to the postsynaptic potential are small. The focus of this review is upon the mathematical techniques that give the time distribution of output spikes, namely stochastic differential equations and the Fokker–Planck equation. The integrate-and-fire neuron model has become established as a canonical model for the description of spiking neurons because it is capable of being analyzed mathematically while at the same time being sufficiently complex to capture many of the essential features of neural processing. A number of variations of the model are discussed, together with the relationship with the Hodgkin–Huxley neuron model and the comparison with electrophysiological data. A brief overview is given of two issues in neural information processing that the integrate-and-fire neuron model has contributed to – the irregular nature of spiking in cortical neurons and neural gain modulation.

Keywords Integrate-and-fire neuron · Neural models · Conductance models

A. N. Burkitt (✉)
The Bionic Ear Institute, 384–388 Albert Street,
East Melbourne, VIC 3002, Australia
E-mail: aburkitt@bionicear.org

A. N. Burkitt
Department of Electrical and Electronic Engineering,
The University of Melbourne,
Melbourne, VIC 3010, Australia

1 Introduction

The integrate-and-fire neuron model has both a long history (Lapicque 1907) and wide application (Tuckwell 1988a). Lapicque (1907) put forward a model of the neuron membrane potential in terms of an electric circuit consisting of a resistor and capacitor in parallel, representing the leakage and capacitance of the membrane. In this model the membrane capacitor is charged until it reaches a certain threshold, at which time it discharges, producing an action potential (spike) and the potential is reset. This simple deterministic model enabled Lapicque to calculate the spiking-rate of a neuron that was coupled to a fixed-voltage stimulating electrode. A more extensive analysis of Lapicque's model with injected current was carried out by Hill (1936). One of the key insights into neural behavior that this approach captures is the separation in time scale of the relatively slow subthreshold integration and the very rapid spike generation. Rather than being an oversimplification, this approach has been very useful because the rapid voltage change during spike generation is extremely stereotypical. Focusing upon the subthreshold membrane properties and excluding the mechanisms responsible for generating action potentials (i.e., the voltage-dependent sodium and potassium channels) has proven to be a powerful tool in understanding the information processing capabilities of neurons.

However, in order to model in vivo neurons, it is necessary to take into account the apparently random times of arrival of the synaptic inputs. The earliest solution of the integrate-and-fire model that incorporated stochastic activity modeled the incoming postsynaptic potentials (PSPs) as a random walk (Gerstein and Mandelbrot 1964). Subsequent developments have largely built upon this diffusion approach using stochastic differential equations and the Ornstein–Uhlenbeck process (Uhlenbeck and Ornstein 1930). Stein formulated the integrate-and-fire model with stochastic input to include the decay of the membrane potential (Stein 1965, 1967), and a number of other authors have subsequently investigated the model using both stochastic differential equations and numerical techniques (Knight 1972; Kryukov 1976;

Tuckwell 1977; Wilbur and Rinzel 1982; Lánský 1984). These techniques have further been used to examine the role of inhibition in the Stein model (Tuckwell 1978a; Cope and Tuckwell 1979; Tuckwell and Cope 1980) and a number of other features such as the effect of reversal potentials (Tuckwell 1979; Wilbur and Rinzel 1983; Hanson and Tuckwell 1983; Musila and Lánský 1994).

The Hodgkin–Huxley model (Hodgkin and Huxley 1952) describes the neuron membrane potential in terms of the dynamic behavior of the various ion channels of the soma and dendrites. The increasing computational resources that have become available in recent years mean that it is not only possible to numerically simulate Hodgkin–Huxley model neurons with dozens of types of ion channels and hundreds of spatial compartments, but it is also possible to investigate the behavior of small networks of such neurons. However, such complex computational models suffer a number of limitations. First, it is frequently difficult to deduce, or gain an intuitive understanding of, the essential nature of the neuronal dynamics observed in these models. Second, they contain so many parameters that it is frequently difficult to make any meaningful exploration of the available parameter space, and thereby have any certainty about the robustness of the observed phenomena. Third, such models cannot be analyzed analytically, but rather they can only be analyzed using the results of numerical simulations, which are subject to statistical errors that may make it difficult to interpolate or extrapolate meaningfully the result of varying a parameter. Consequently, the large amount of detail contained in these models can often obscure rather than illuminate the essential underlying principles governing the information processing carried out by large numbers of interconnected neurons.

This review is concerned primarily with the mathematical techniques available to analyze the integrate-and-fire neuron model, although results from computer simulations will also be mentioned since these play an important role in supporting the analytical studies and addressing questions that are still beyond the reach of analytical methods. The integrate-and-fire neuron model is introduced in Sect. 2, giving details of the synaptic input and the solution for injected current, as well as some variants of the basic model. Stochastic models are discussed in Sect. 3, including the diffusion model, the Weiner process, the Stein model, the Ornstein–Uhlenbeck process, the Gaussian approximation, and the Fokker–Planck equation. The solution of the model with homogeneous Poisson input and both current and conductance synapses is presented in Sect. 4, where the interspike interval distribution is given by the solution for the first passage time problem using the renewal equation. The output spiking-rate is given, as is the stationary solution for the membrane potential distribution. Extensions of the basic model are discussed in Sect. 5, including finite synaptic time constants, correlated synaptic input, and adaptation effects. The relationship between the Hodgkin–Huxley and integrate-and-fire neuron models is discussed in Sect. 6, together with the comparison of the models to physiological data. The application of the model to two major issues in neural information processing is discussed in Sect. 7, namely the variability of neural responses and neural gain modulation. The case in which the synaptic inputs are time-dependent (i.e., described by a temporally inhomogeneous Poisson processes), is reviewed in the accompanying paper (Burkitt 2006). This review builds upon, and is indebted to, earlier reviews of these models (Ricciardi 1977; Ricciardi and Sacerdote 1979; Tuckwell 1988b; Lánský and Sato 1999).

2 The integrate-and-fire neuron model

In the integrate-and-fire neuron model the state of the neuron is characterized by its membrane potential. The membrane potential receives excitatory or inhibitory contributions by synaptic inputs that arrive from other neurons by their associated synapses. These inputs, that are each weighted by their respective synaptic strength, are modeled either as injected current (*current synapse* models in which summation is linear) or as a change in the membrane conductance (*conductance synapse* models in which summation of the synaptic input is nonlinear, i.e., the amplitude depends upon the value of the membrane potential). Conductance synapse models take account of the change in amplitude of the excitatory and inhibitory inputs, which depends upon the difference between the membrane potential and the corresponding reversal potential. The integrate-and-fire neuron model is a point neuron (single compartment) model in which the spatial structure of the neuron associated with the dendrites is neglected.

The neuron is leaky since the summed contributions to the membrane potential decay with a characteristic time constant (the membrane time constant). If this decay of the membrane potential over time is neglected, the model is a *perfect integrator* (Gerstein and Mandelbrot 1964). When the membrane potential reaches a (fixed) threshold, an output spike is generated–the *integrate-and-fire* mechanism. The interspike intervals (ISIs) of the resulting action potentials are, therefore, identified as the *first passage time* of the membrane potential, $v(t)$, across the threshold, $V_{\rm th}$. One of the main goals of the mathematical analysis of the model with stochastic synaptic input is to evaluate the first passage time distribution, $f_\theta(t)$, from which the other properties of the output spike distribution can be deduced. After the membrane potential crosses threshold it is reset to its resting value and is inactivated for a brief time corresponding to the absolute refractory period of the neuron.

The model is described by the dynamics of the neuron's membrane potential, $v(t)$,

$$C_{\rm m}\frac{{\rm d}v(t)}{{\rm d}t} = I_{\rm leak}(t) + I_{\rm s}(t) + I_{\rm inj}(t), \qquad (1)$$

where $C_{\rm m}$ is the membrane capacitance, $I_{\rm leak}(t)$ is the current due to the passive leak of the membrane, $I_{\rm s}(t)$ is a current describing the effect of synaptic input to the neuron, and $I_{\rm inj}(t)$ is a current injected into the neuron (by an intracellular electrode). The leak current is

$$I_{\text{leak}}(t) = -\frac{C_{\text{m}}}{\tau_{\text{m}}}[v(t) - V_0], \tag{2}$$

where V_0 is the resting potential and τ_{m} is the passive membrane time constant, which is related by $\tau_{\text{m}} = R_{\text{m}}C_{\text{m}}$ to the capacitance and the leak resistance, R_{m}, of the membrane potential, both of which are assumed to be constant.

The generation of an action potential when the membrane potential reaches the spiking threshold is generally not considered an intrinsic part of the model. Consequently, it is usual in the description of integrate-and-fire neurons to only describe the sub-threshold membrane voltage. Nevertheless, it is possible to formally include the spiking mechanism in terms of a *spiking current* I_{spike} (Meffin et al. 2004),

$$I_{\text{spike}}(t) = C_{\text{m}}\left[\frac{\mathrm{d}v(t)}{\mathrm{d}t}\right]^{-1}_{v=V_{\text{th}}}(V_{\text{reset}} - V_{\text{th}})\delta[v(t) - V_{\text{th}}], \tag{3}$$

which describes a spike when the membrane potential reaches the spike generating threshold, V_{th}, and subsequently the membrane potential resets to V_{reset} ($\delta(.)$ denotes the Dirac delta function). The membrane potential begins to evolve again according to Eq. (1) after an absolute refractory period, τ_{r}.

2.1 Synaptic input to integrate-and-fire neurons

Before examining the input–output relationship of the model, it is necessary to define the synaptic input, which may be modeled in two ways: as current synapses or conductance synapses.

2.1.1 Current synapses

The synaptic current for a current synapse is independent of the membrane potential and is described by

$$I_{\text{s}} = C_{\text{m}}\sum_{k=1}^{N_{\text{E}}} a_{\text{E},k}S_{\text{E},k}(t) + C_{\text{m}}\sum_{k=1}^{N_{\text{I}}} a_{\text{I},k}S_{\text{I},k}(t), \tag{4}$$

where the amplitudes, $a_{\text{E},k} > 0$ and $a_{\text{I},k} < 0$, are the change in potential due to a single synaptic event; the associated charge delivered to the neuron by an excitatory and inhibitory synaptic input is $C_{\text{m}}a_{\text{E},k}$ and $C_{\text{m}}a_{\text{I},k}$, respectively. $S_{\text{E},k}(t)$, and $S_{\text{I},k}(t)$ describe, respectively, the excitatory and inhibitory synaptic inputs as a series of input spikes to each synapse

$$S_{\text{E},k}(t) = \sum_{t_{\text{E},k}}\delta(t - t_{\text{E},k}), \quad S_{\text{I},k}(t) = \sum_{t_{\text{I},k}}\delta(t - t_{\text{I},k}), \tag{5}$$

where $t_{\text{E},k}$ and $t_{\text{I},k}$ are the times of the synaptic input spikes for the excitatory and inhibitory synapses, respectively. These input spikes are usually modeled as Poisson processes with individual excitatory and inhibitory synaptic input intensities (i.e., spiking-rates), $\gamma_{\text{E},k}$ and $\gamma_{\text{I},k}$, respectively. In this review only homogeneous Poisson processes, in which these spiking-rates are constant, are considered. The more general case in which the Poisson spiking-rates are time dependent (i.e., temporally inhomogeneous Poisson processes), is reviewed in the accompanying paper (Burkitt 2006). The pooled Poisson processes associated with the N_{E} excitatory and N_{I} inhibitory synaptic inputs are denoted by $S_{\text{E}}(t)$ and $S_{\text{I}}(t)$,

$$S_{\text{E}}(t) = \sum_k S_{\text{E},k}(t), \quad S_{\text{I}}(t) = \sum_k S_{\text{I},k}(t), \tag{6}$$

with spiking-rates λ_{E} and λ_{I}, respectively, as discussed further in Sect. 3. A single integrate-and-fire neuron with current synapses is illustrated in Fig. 1, which shows the N_{E} excitatory and N_{I} inhibitory synapses. The inputs are summed linearly and output spikes are represented as δ-functions at the times when the membrane potential crosses threshold.

The resultant change to the membrane potential (the EPSP or IPSP) of the total δ-function synaptic input is shot-noise (Papoulis 1991). The contribution of a single δ-function input upon the membrane potential, called the (normalized) postsynaptic response function, is given by

$$\varepsilon(t) = \frac{1}{\tau_{\text{m}}}\mathrm{e}^{-t/\tau_{\text{m}}}\Theta(t), \tag{7}$$

where the Heaviside step function $\Theta(t)$ ensures causality.

In order to take account of the synaptic dynamics, it is necessary to go beyond the simple δ-function synaptic input and consider an input current with a finite time constant

$$I_{\text{s}} = \frac{a_{\text{E}}C_{\text{m}}}{\tau_{\text{s}}}\mathrm{e}^{-t/\tau_{\text{s}}}\Theta(t), \tag{8}$$

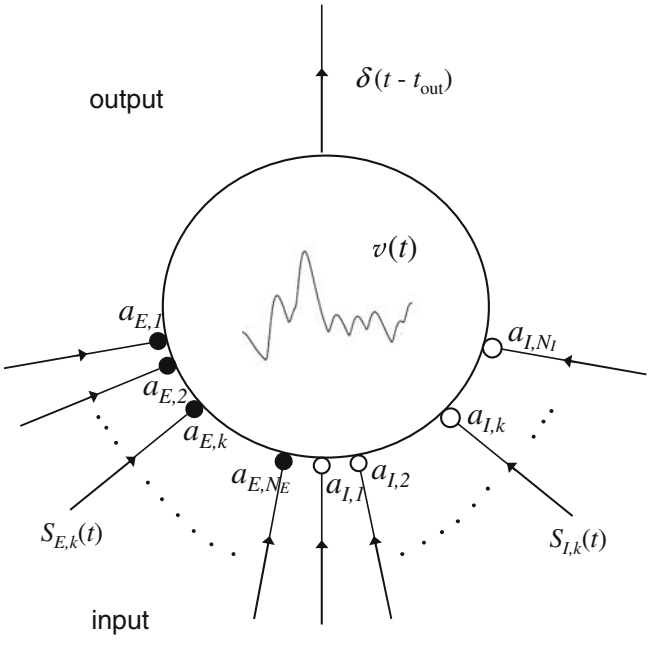

Fig. 1 Schematic representation of an integrate-and-fire neuron with N_{E} excitatory (*filled circles*) and N_{I} inhibitory (*open circles*) current synapses. Each excitatory (inhibitory) synapse receives an input spike train denoted by $S_{\text{E},k}(t)$ ($S_{\text{E},k}(t)$). The subthreshold membrane voltage, $v(t)$, is the sum of the EPSPs and IPSPs, a portion of which is illustrated here with the postsynaptic response function of Eq. (9). Output spikes are δ-functions, generated when the membrane potential reaches threshold

where τ_s is the *synaptic time constant* (in general different for each type of neuron). This gives a normalized postsynaptic response function of the form

$$\varepsilon(t) = \frac{(e^{-t/\tau_m} - e^{-t/\tau_s})}{(\tau_m - \tau_s)}\Theta(t). \tag{9}$$

Other forms of synaptic current input can be considered, such as the α-function, $I_s \propto te^{-\alpha t}$ (Jack et al. 1985), which can be used to model the filtering effect of the dendritic tree upon the voltage at the soma. Methods to include finite synaptic time constants in the integrate-and-fire neuron model with current synapses are discussed further in Sect. 5.1.

2.1.2 Conductance synapses

A more biologically accurate description of the synaptic current is given by (cf. Eq. 4) (Tuckwell 1979, 1988b)

$$I_s(t) = C_m[V_E - v(t)]\sum_{k=1}^{N_E} g_{E,k}S_{E,k}(t) + C_m[V_I - v(t)]\sum_{k=1}^{N_I} g_{I,k}S_{I,k}(t). \tag{10}$$

The potentials V_E and V_I are the (constant) reversal potentials ($V_I \leq V_{reset} < V_{th} < V_E$). The reversal potentials arise from the equilibrium potentials of the ion channels and are so named because the direction of associated current flow switches when the membrane potential passes through the corresponding reversal potential. The reversal potentials introduce a nonlinearity into the summation of the individual synaptic inputs. The parameters $g_{E,k}, g_{I,k} > 0$ are taken to be small in this model and represent the integrated inhibitory and excitatory conductances over the time course of the synaptic event divided by the neural capacitance and are thus dimensionless (they are nonnegative and for convenience are taken here to be identical for all excitatory and inhibitory inputs, respectively, so that the subscripts k in the above equation are subsequently dropped). The excitatory synaptic conductance g_E is identified with the synaptic weight and the two terms are used interchangeably in the literature on synaptic plasticity.

In this model, the synaptic current inputs are often taken to have the form of δ-functions, as discussed above for current synapses. The reason for this is that a finite synaptic time constant introduces temporal correlations in the membrane voltage, as it does for current synapses. The nonlinear summation of synaptic input with conductance synapses makes the analysis much more difficult as becomes apparent when the renewal equation, Eq. (24), is introduced. Including finite synaptic time constants in the integrate-and-fire neuron model with conductance synapses is discussed further in Sect. 5.1.

2.2 Deterministic input to integrate-and-fire neurons

The subthreshold membrane voltage under the influence of a deterministic injected current $I_{inj}(t)$ is described by Eq. (1), where the synaptic input is neglected and the leak current is given by Eq. (2). For subthreshold potentials the solution of this differential equation is (Tuckwell 1988a)

$$v(t) = V_0 + e^{-t/\tau_m}\int_{t_0}^{t} \frac{I_{inj}(t')}{C_m} e^{t'/\tau_m} dt', \tag{11}$$

where it is assumed that the membrane potential at the initial time t_0 is at the resting potential $v(t_0) = V_0$. When the membrane potential reaches the threshold, a spike is generated. Immediately following the spike, the membrane potential is reset to its initial value V_{reset}. Refractory effects may be included by allowing the threshold to become infinite immediately following the generation of a spike, corresponding to an absolute refractory period τ_r. A relative refractory period may be included by introducing a time dependence to the threshold, so that it has an elevated value for a limited time immediately following a spike, as discussed further in Sect. 5.3.

For a fixed threshold and constant injected current I the membrane potential following reset at time t_0 evolves according to

$$v(t) = V_0 + IR_m\left(1 - e^{-(t-t_0)/\tau_m}\right). \tag{12}$$

For simplicity the reset potential is taken to be the resting potential, $V_{reset} = V_0$, throughout. The time it takes for a spike to be generated (i.e., the interspike interval, T_{ISI}) is

$$T_{ISI} = -\tau_m \ln\left[1 - \frac{\theta}{IR_m}\right], \quad (IR_m > \theta), \tag{13}$$

where $\theta = (V_{th} - V_0)$ is the potential difference between the spike generating threshold and the resting potential. This expression for T_{ISI} is only valid for $(IR_m) > \theta$, otherwise the potential does not reach threshold and there is no output spike. From this relationship the strength-duration curve can be derived, which gives the time required for an input current of a fixed amplitude to generate a spike (Noble and Stein 1966). The corresponding spiking-rate is given by

$$\lambda_{out} = (\tau_r + T_{ISI})^{-1}, \tag{14}$$

where τ_r is the absolute refractory period during which all input current is assumed to be lost. For large currents the time to spike is $T_{ISI} = \tau_m\theta/(IR_m)$, giving an approximately linear regime when $\tau_r \ll T_{ISI}$. For very large currents the output spiking-rate saturates at the inverse of the absolute refractory period. For currents below a threshold current $I_{th} = \theta/R_m$ there will be no output spikes. A peculiarity of the integrate-and-fire neuron model is that the slope of the input–output curve (i.e., λ_{out} as a function of I) has a singularity at $I = I_{th}$.

These properties of the model with deterministic input are relatively straightforward and the real interest with integrate-and-fire neuron models is in taking account of stochastic inputs, which is discussed in the following section.

2.3 Variants of the integrate-and-fire neuron model

A variation of the integrate-and-fire neuron model is the spike response model (Gerstner 1995, 2001; Gerstner and Kistler 2002). The motivation for the spike response model lies in the difficulty of finding analytic solutions of the diffusion-type integrate-and-fire neuron models, especially when inhomogeneous Poisson synaptic input is considered. In the spike response model, the membrane potential explicitly depends upon the time of the last spike. This time dependence enables the refractory properties of the neuron to be modeled, including a reduced responsiveness and increased threshold after the generation of a spike, as well as a hyperpolarizing spike-afterpotential. One essential difference to the conventional integrate-and-fire neuron model, Eq. (1), is that the reset of the membrane potential after spike generation is achieved by adding to the membrane potential an additional "afterpotential" term $\eta(t - t_f)$ (where t_f is the time of firing of the previous spike). This term explicitly describes the time course of the action potential and the afterpotential. The model also includes a dynamic threshold that is elevated after a spike is generated (similar variable threshold models for including refractory effects in integrate-and-fire neuron models are discussed in Sect. 5.3). The leaky integrate-and-fire neuron model is a special case of the spike response model, in which the afterpotential function $\eta(t)$ is a shot-noise function: $\eta(t) = (V_{reset} - V_{th}) \exp[-(t - t_f)/\tau_m]\Theta(t - t_f)$ (in the case of conductance synaptic input the time constant must be set to the effective membrane time constant, as discussed in Sect. 4.2). In order to examine inhomogeneous Poisson synaptic input using the spike response model, an escape process is introduced that is completely described by a hazard function, which depends only on the momentary values of the membrane potential and input current (Cox and Lewis 1966). An appropriate choice of hazard function has been shown to reproduce both the generation of individual spikes and more complex properties seen in integrate-and-fire neurons (Plesser and Gerstner 2000).

Other variations of the model include; the linear integrate-and-fire neuron (Fusi and Mattia 1999), in which the subthreshold membrane potential depolarization is constant (i.e., $I_{leak}(t)$ in Eq. (1) is a constant), the quadratic integrate-and-fire neuron (Ermentrout and Kopell 1986; Latham et al. 2000; Brunel and Latham 2003; Lindner et al. 2003), in which there is a nonlinear leakage term $V^2(t)$ on the right of Eq. (1), the exponential integrate-and-fire neuron (Fourcaud-Trocmé et al. 2003; Fourcaud-Trocmé and Brunel 2005), in which there is a term that has an exponential dependence upon $V(t)$ on the right of Eq. (1), and the generalized integrate-and-fire neuron (Richardson et al. 2003; Brunel et al. 2003), which allows the description of subthreshold resonance. The quadratic integrate-and-fire neuron model represents the canonical form of a neuron in which spikes are generated by a type I bifurcation (Izhikevich 1999) and it is related to the θ-neuron by a change of variables (Ermentrout 1996; Gutkin and Ermentrout 1998). A discussion of both the biological plausability and the computational efficiency of a number of widely used spiking neuron models is given by Izhikevich (2004).

3 Methods of analysis for stochastic models

In general, there are two sources of noise associated with the neural membrane potential: one *intrinsic* to the neuron, associated with such properties as the stochastic nature of the underlying mechanisms controlling the release of neurotransmitter and the opening of channels, and the other *external* to the neuron, arising from the apparently random arrival times of the inputs. The representation of the neuron as a point (i.e., a single compartment) means that there is no clear distinction between these two sources of noise, which can be treated together in terms of the variance of the fluctuations in the membrane potential. Intracellular recordings of neurons indicate that the internal noise is generally insignificant in comparison with that associated with the stochastic synaptic input (Calvin and Stevens 1968; Bryant and Segundo 1976; Mainen and Sejnowski 1995).

Consequently, the predominant source of randomness in the model is the stochastic arrival times of the synaptic input, and these are generally (indeed almost universally) modeled as a Poisson process (Cox 1962; Cox and Miller 1965). While the inputs to a single synapse may differ significantly from a Poisson process, so long as they can be adequately described as a renewal process (i.e., the successive time intervals between inputs are independent and identically distributed) and the inputs are independent, the *pooling property* of independent renewal processes provides an excellent description of the combined input of a large number of synapses. The pooling property, also called the superposition property, is implicit in Eq. (6) and ensures that the statistical properties of the combined process is "locally random", in the sense that it will appear random over periods of time that are small compared to the individual mean interspike times (Cox and Smith 1954). In general, the pooled process provides a very good description of the combined input to a neuron when the number of input synapses is increased to even a moderate number. One of the first papers to discuss in depth the relationship between spike trains and stochastic point processes (i.e., stochastic processes described as a series of point events in time) was Perkel et al. (1967), and for a more recent discussion of the Poisson process description of synaptic input see Johnson (1996). A description of the pooled spike train, obtained from superposing the spike trains of individual synapses, as a cluster point process is given in Gomez et al. (2005), together with the physiological ramifications of this hypothesis. A recent study of both inter-spike variability and long-range dependence showed that in certain situations it may be more accurate to describe the synaptic inputs in terms of fractional-Gaussian-noise-driven Poisson processes, rather than renewal point processes (Jackson 2004). The situation in which the inputs are not independent, but rather have a temporal correlation, is discussed in Sect. 5.2.

The general formulation of the stochastic integrate-and-fire neuron model is given in the remainder of this section, in which the techniques and methods used in its solution are outlined. Details of the solutions and results are given in the following section in the case where the synaptic input is a homogeneous Poisson process (Sect. 4).

3.1 Diffusion models

The diffusion models of neurons treat the membrane potential as a *diffusion process*, namely as a continuous-time Markov process with a continuous path (Tuckwell 1988b). The stochastic nature of the synaptic input may be described by modeling the membrane potential, Eq. (1), as a stochastic differential equation, called the Ornstein–Uhlenbeck model (Uhlenbeck and Ornstein 1930), with mean input μ (taken to be constant for homogeneous synaptic input) and a Gaussian white noise $\xi(t)$ with intensity coefficient σ

$$\tau \frac{\mathrm{d}v(t)}{\mathrm{d}t} = -[v(t) - V_0] + \mu + \sigma\sqrt{2\tau}\xi(t), \tag{15}$$

where $\langle \xi(t) \rangle = 0$ and $\langle \xi(t)\xi(t') \rangle = \delta(t - t')$ (note that some authors use alternative notations in which the τ dependence on the rhs is absorbed into either the definition of σ or ξ). For simplicity, it will be assumed throughout that the membrane potential at the initial time t_0 is at the resting potential V_0 and that this is also the reset potential: $v(t_0) \equiv v_0 = V_0 = V_{\mathrm{reset}}$. The most straightforward way to derive the Ornstein–Uhlenbeck model is via the formulation of Stein (1965), described in Sect. 3.1.2. However, before discussing these models a simpler diffusion neuronal model is introduced, namely the Wiener process.

3.1.1 Random walk model and Wiener process

One of the first stochastic integrate-and-fire neuron models to be analyzed was the *perfect integrator* (or leakless integrate-and-fire neuron model), in which the decay of the membrane potential over time is neglected. This model, analyzed by Gerstein and Mandelbrot (1964), is obtained as the limiting case of the (discontinuous) random walk process (Brownian motion), in which the membrane potential undergoes step changes in amplitude with the arrival of each PSP. By examining the situation in which the amplitude of each step becomes smaller, while at the same time the input rate increases, the trajectory of the membrane potential becomes continuous (the *diffusion approximation*). Such a Wiener process of the membrane potential is described by (Tuckwell 1988b)

$$v(t) = v_0 + \mu_{\mathrm{W}} t + \sigma_{\mathrm{W}} W(t), \quad t > 0, \tag{16}$$

where $v(0) = v_0$ and $W(t)$ is a standard Wiener process with variance parameter σ_{W} and drift parameter $\mu_{\mathrm{W}} > 0$. Note that the step size is required to scale as $\sqrt{\Delta t}$ in the continuum limit and that the generalized derivative of a Wiener process is white noise [for a recent exposition of the Wiener Process see Stirzaker (2005)].

Both the lack of a lower bound on the potential and the neglect of the membrane leakage are unrealistic approximations and limit the usefulness of this model. Nevertheless, it provides a reasonable approximation when there is positive drift and the synaptic inputs summate to threshold over a much shorter time scale than the membrane decay constant τ_{m}. Its analytic tractability makes the model useful in defining the large τ_{m} limit of the more general model. The first passage time density for this model with homogeneous Poisson synaptic input is given in Sect. 4.1.

3.1.2 Stein model and Ornstein–Uhlenbeck process

Stein (1965) described the fluctuations of the membrane potential between two firing events, due to current synaptic input, as a one-dimensional stochastic process described by,

$$\tau_{\mathrm{m}} \frac{\mathrm{d}v(t)}{\mathrm{d}t} = -[v(t) - V_0] + a_{\mathrm{E}} S_{\mathrm{E}}(t) + a_{\mathrm{I}} S_{\mathrm{I}}(t). \tag{17}$$

Each synaptic input gives rise to a change in the membrane potential that is a step discontinuity, and can be modeled as a synaptic response function of the shot-noise form, Eq. (7). The model is illustrated in Fig. 2, which shows the incoming synaptic input, the resulting membrane potential with step discontinuities, and the output spikes generated when the potential reaches threshold. Between subsequent synaptic inputs the potential decays with time course determined by the membrane time constant τ_{m}.

Just as it is possible to construct a continuous version of the discrete random walk model for the perfect integrator model by the Wiener process with drift, Eq. (16), so can a continuous version of Stein's model (which has jumps in the

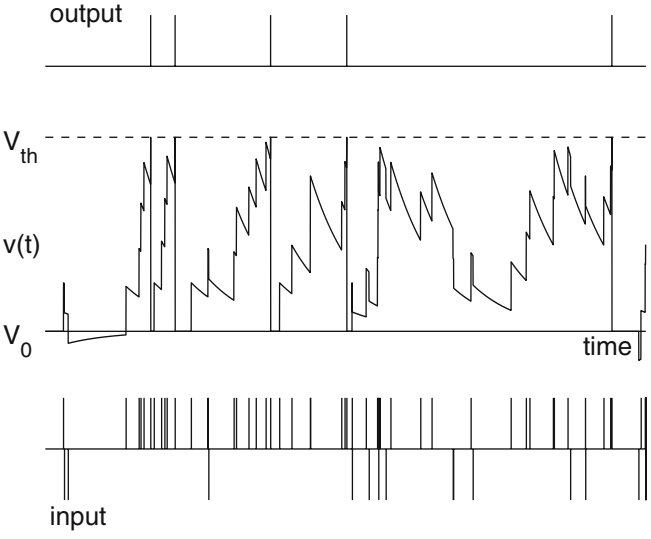

Fig. 2 Illustration of the Stein model with current synapses, showing the relationship between the synaptic input (*bottom plot*), the membrane potential (*middle plot*), and the output spikes (*top plot*) as a function of time. Synaptic inputs *above* and *below* the axis represent excitatory and inhibitory inputs respectively. *Dotted lines* in the middle plot represent threshold (upper dotted line) and the resting potential (taken here to be equal to the reset potential)

potential) be constructed through the Ornstein–Uhlenbeck process, given in Eq. (15). This approach proceeds by constructing a diffusion process with the same first and second moments as the Stein model, as shown in Ricciardi (1976) and Lánský (1984) for homogeneous Poisson processes and in Lánský (1997) for inhomogeneous Poisson processes.

The time-dependent first and second moments, $\mu(t; v_0)$ and $\sigma^2(t; v_0)$, of the *free* or *unrestricted* membrane potential (i.e., neglecting the spiking threshold) are defined by

$$\begin{aligned} \mu(t; v_0) &\equiv \mathrm{E}[v(t)|v_0, t_0 = 0] \\ \sigma^2(t; v_0) &\equiv \mathrm{Var}[v(t)|v_0, t_0 = 0]. \end{aligned} \tag{18}$$

Their evaluation requires the expectation value of a Poisson process: a process $S(t)$ with intensity λ has expectation values over the time interval Δt given by

$$E\left[S(t + \Delta t)\right] = E\left[S^2(t + \Delta t)\right] = \lambda \Delta t + o(\Delta t). \tag{19}$$

In the case of current synapses with homogeneous Poisson input, the first and second moments of the free membrane potential are

$$\begin{aligned} \mu(t; v_0) &= v_0 \mathrm{e}^{-t/\tau_\mathrm{m}} + \mu_\mathrm{Q}(1 - \mathrm{e}^{-t/\tau_\mathrm{m}}) \\ \sigma^2(t; v_0) &= \sigma_\mathrm{Q}^2(1 - \mathrm{e}^{-2t/\tau_\mathrm{m}}), \end{aligned} \tag{20}$$

where the large time (equilibrium) limits of the mean and variance of the free membrane potential are identified as the drift and diffusion coefficients of the Ornstein–Uhlenbeck process

$$\begin{aligned} \tau &= \tau_\mathrm{m} \\ \mu &= \mu_\mathrm{Q} \equiv \tau_\mathrm{m}\left(a_\mathrm{E}\lambda_\mathrm{E} - a_\mathrm{I}\lambda_\mathrm{I}\right) \\ \sigma^2 &= \sigma_\mathrm{Q}^2 \equiv \frac{\tau_\mathrm{m}}{2}\left(a_\mathrm{E}^2\lambda_\mathrm{E} + a_\mathrm{I}^2\lambda_\mathrm{I}\right). \end{aligned} \tag{21}$$

This correspondence between the first two moments of the Stein model and the drift and variance of the Ornstein–Uhlenbeck process requires that the limits are taken in the appropriate manner (Lánský 1984). Consequently, the membrane potential approaches an equilibrium value, μ_Q, about which it fluctuates with variance σ_Q^2. The results for homogeneous Poisson synaptic input with conductance synapses are given in Sect. 4.

The diffusion approximation has been very successful in describing the Stein model when the synaptic input can be modeled as Gaussian white noise. However, when finite synaptic time constants or temporal correlations are introduced the noise is colored and alternative methods such as the Fokker–Planck formalism have proved more successful, as described in Sect. 3.2.

3.1.3 Gaussian approximation

An alternative formulation uses the Gaussian approximation, which proceeds by considering the evolution of the free membrane potential. The conditional probability density of the free membrane potential $p(v, t|v_0, t_0)$, which is the probability that it has the value v at time t given that it had the value v_0 at some earlier time t_0, is parameterized as (Burkitt and Clark 2000)

$$p(v, t|v_0, 0) = \frac{1}{\sqrt{2\pi\sigma^2(t; v_0)}} \exp\left\{-\frac{[v - \mu(t; v_0)]^2}{2\sigma^2(t; v_0)}\right\}, \tag{22}$$

where $\mu(t; v_0)$ and $\sigma^2(t; v_0)$ are given by Eq. (18). These values are evaluated using a self-consistent formalism in which the mean and variance are calculated by evaluating the first two moments of the corresponding Gaussian distribution. The Gaussian approximation is accurate in the limit of a large number of small-amplitude synaptic inputs, as can be shown using the central limit theorem (Lamperti 1966, 1996). The error scales as $1/\sqrt{N}$, as also found in a related study (Kempter et al. 1998). Comparisons of the simulated probability density of the free membrane potential and the Gaussian approximation show an excellent match between analytical approximation and computer simulation (Hohn and Burkitt 2001). The Gaussian approximation, although equivalent to the diffusion approximation, has proven to be particularly useful in the study of the integrate-and-fire neuron model with conductance synapses (Burkitt 2001).

3.1.4 Stein model with conductance synapses

The Stein model with conductance synapses is described by (Tuckwell 1979, 1988b) [cf. Eq. (10)]

$$\begin{aligned} \tau_\mathrm{m}\frac{\mathrm{d}v(t)}{\mathrm{d}t} &= -[v(t) - V_0] + g_\mathrm{E}[V_\mathrm{E} - v(t)]S_\mathrm{E}(t) \\ &\quad + g_\mathrm{I}[V_\mathrm{I} - v(t)]S_\mathrm{I}(t). \end{aligned} \tag{23}$$

Note that the discontinuous jumps associated with each synaptic input are now *state dependent*, i.e., the jump size depends upon the value of the membrane potential. This results in a nonlinear summation of the individual excitatory and inhibitory PSPs, whereby the amplitude of the PSP decreases according to how close the membrane potential is to the corresponding reversal potential. The leakage term is often conveniently written in terms of the passive leakage conductance $g_\mathrm{L} = 1/R_\mathrm{m}$.

A number of variations of this model have been investigated (Hanson and Tuckwell 1983; Wilbur and Rinzel 1983; Smith and Smith 1984; Kallianpur and Wolpert 1987; Lánský and Lánská 1987; Lánský and Musila 1991; Lánský and Smith 1991; Musila and Lánský 1994; Lánská et al. 1994; Lánský et al. 1995; Lánská and Lánský 1998). As for the Stein model with current synapses, the discontinuous nature of the trajectory of the membrane potential, together with the nonlinear summation of the PSPs, complicates the analytical study of this model. It is therefore convenient to analyze the corresponding diffusion model, i.e., the diffusion model with statistically equivalent properties. The solution with homogeneous Poisson input is discussed in Sect. 4.2.

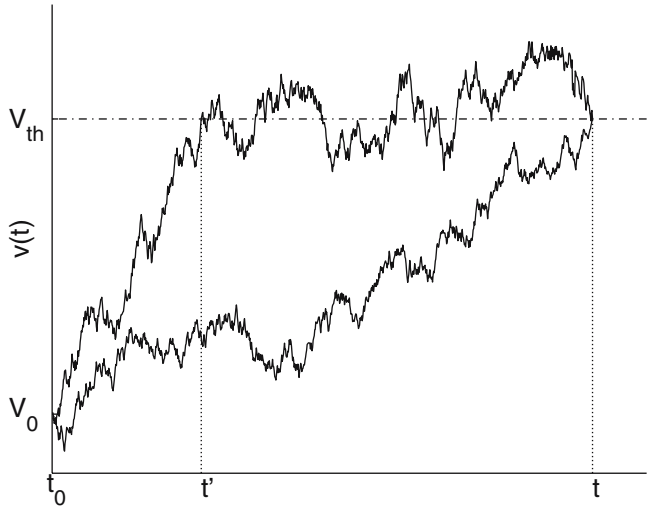

Fig. 3 Illustration of the renewal Eq. (24). The conditional probability density that the membrane potential $p(V_{\rm th}, t|V_{\rm reset}, t_0)$ will have the value $V_{\rm th}$ at time t, given that it had the value v_0 at an earlier time t_0, is obtained by integrating over all paths linking $v(t_0^+) = V_{\rm reset}$ with $v(t^-) = V_{\rm th}$. Splitting each path into the first approach to threshold (indicated for the upper trajectory by time t') and the return to threshold (at time t) yields the renewal Eq. (24) [taken from Burkitt and van Hemmen 2003]

3.1.5 Renewal equation

In the diffusion and Gaussian approximations to the integrate-and-fire neuron model, the quantity that emerges naturally from the calculation is the time at which the membrane potential, $v(t)$, crosses the threshold, $V_{\rm th}$, for the first time. This first passage time density, $f_\theta(t)$, represents the output interspike interval distribution and obeys the renewal equation (Plesser and Tanaka 1997; Burkitt and Clark 1999)

$$p(V_{\rm th}, t|v_0, t_0) = \int_{t_0}^{t} {\rm d}t' f_\theta(t') p(V_{\rm th}, t|V_{\rm th}, t'), \tag{24}$$

where $p(v, t|v', t')$ is the conditional probability density of the membrane potential defined above in the description of the Gaussian approximation. This formulation of the first passage time problem, illustrated in Fig. 3, is due to Schrödinger (1915) and involves splitting the trajectory of the freely evolving membrane potential into two sections: the first approach to threshold at time t' and the later return to threshold at time t. This equation is exact for synaptic input modeled as a series of δ-functions; otherwise it is approximate, since finite synaptic time constants introduce temporal correlations (Sect. 5.1) that destroy the renewal property of the equation.

The integral in Eq. (24) can be solved using the convolution theorem of Laplace transforms, where the Laplace transform $f_{\theta,{\rm L}}(s) = \mathcal{L}\{f_\theta(t)\}$ is obtained using the time-translation invariance $p(v, t|v_0, t_0) = p(v, t-t_0|v_0, 0)$, which depends upon the inputs being a homogeneous Poisson process.

3.2 Fokker–Planck formalism

An alternative formalism is the Fokker–Planck equation, which describes the time evolution of the probability density $P(v, t)$ of the membrane potential (van Kampen 1992; Risken 1996)

$$\frac{\partial}{\partial t} P(v, t) = \left[-\frac{\partial}{\partial v} A(v) + \frac{1}{2} \frac{\partial^2}{\partial v^2} B(v) \right] P(v, t), \tag{25}$$

where $A(v)$ is the drift function and $B(v)$ is the diffusion function, which are the first two zero centered moments of the distribution of the independent jumps in the membrane potential due to the stochastic synaptic input. For the Ornstein–Uhlenbeck process with current synapses, Eq. (15), these functions are given by (Brunel and Hakim 1999)

$$A(v) = -\frac{1}{\tau}(v - V_0 - \mu), \quad B(v) = \frac{2\sigma^2}{\tau}, \tag{26}$$

where τ, μ, and σ are given in Eq. (21). The Fokker–Planck equation can be split into a continuity equation for the probability density

$$\frac{\partial}{\partial t} P(v, t) = -\frac{\partial J(v, t)}{\partial v}, \tag{27}$$

and a constitutive equation for the probability flux $J(v, t)$

$$\begin{aligned} J(v, t) &= A(v)P(v, t) - \frac{1}{2}\frac{\partial}{\partial v} B(v)P(v, t) \\ &= -\frac{1}{\tau}(v - \mu)P(v, t) - \frac{\sigma^2}{\tau}\frac{\partial}{\partial v} P(v, t) \end{aligned} \tag{28}$$

which gives the probability current through v at time t (Risken 1996). The instantaneous spiking-rate is given by the flux through the threshold

$$\lambda_{\rm out}(t) = J(V_{\rm th}, t). \tag{29}$$

The boundary conditions need to be specified; at the lower boundary the conditions are

$$\lim_{v \to -\infty} P(v, t) = 0, \quad \lim_{v \to -\infty} vP(v, t) = 0, \tag{30}$$

at the threshold, $V_{\rm th}$, there is an absorbing boundary condition

$$P(V_{\rm th}, t) = 0, \quad \frac{\partial}{\partial v} P(V_{\rm th}, t) = -\frac{\lambda_{\rm out}(t)\tau_{\rm m}}{\sigma^2}, \tag{31}$$

and at the reset potential, $V_{\rm reset}$, the flux from the threshold flows in as a result of the reset mechanism

$$J(V_{\rm reset}^+, t) - J(V_{\rm reset}^-, t) = \lambda_{\rm out}(t - \tau_{\rm r}). \tag{32}$$

The probability distribution also has to satisfy the normalization condition

$$\int_{-\infty}^{V_{\rm th}} {\rm d}v P(v, t) + p_{\rm r}(t) = 1, \tag{33}$$

where $p_{\rm r}(t) = \int_{t-\tau_{\rm r}}^{t} {\rm d}u \lambda_{\rm out}(u)$ is the probability of the neuron being refractory at time t. The generalization of these equations to the situation where there are different populations of excitatory and inhibitory synaptic inputs is straightforward (Brunel 2000).

For the integrate-and-fire neuron model with conductance synapses, the drift and diffusion functions $A(v)$ and $B(v)$ are (Richardson 2004)

$$\begin{aligned} A(v) &= -\frac{1}{\tau_{\rm m}}(v - V_0) + \lambda_{\rm E} g_{\rm E}(V_{\rm E} - v) + \lambda_{\rm I} g_{\rm I}(V_{\rm I} - v) \\ B(v) &= \lambda_{\rm E} g_{\rm E}^2 (V_{\rm E} - v)^2 + \lambda_{\rm I} g_{\rm I}^2 (V_{\rm I} - v)^2. \end{aligned} \tag{34}$$

The Fokker–Planck approach is particularly useful for obtaining the stationary distribution of the membrane potential $P_0(v)$ (Brunel and Hakim 1999; Brunel 2000), which is given by the solution of

$$J_0(v) = A(v)P_0(v) - \frac{1}{2}\frac{\partial}{\partial v}B(v)P_0(v) = C, \tag{35}$$

where C is a constant that is determined by the normalization of the probability distribution. In addition, the Fokker–Planck formalism enables a systematic perturbative expansion that has proven useful in the study of the integrate-and-fire neuron model with finite synaptic time constants and temporal correlations (Brunel and Sergi 1998; Fourcaud and Brunel 2002), as discussed in Sects. 5.1 and 5.2.

4 The spiking-rate and interspike interval distribution

Here, the derivation of the output spiking-rate for temporally homogeneous Poisson inputs is reviewed. How these methods can be extended to the case where the inputs are described by an inhomogeneous Poisson process is reviewed in Burkitt (2005). The output spiking-rate is determined from the average interspike interval, $\overline{T}_{\rm ISI}$, which is the first moment of the first passage time density,

$$\begin{aligned} \lambda_{\rm out} &= \left[\tau_{\rm r} + \overline{T}_{\rm ISI}\right]^{-1} \\ \overline{T}_{\rm ISI} &= {\rm E}[T_{\rm ISI}] = \int_0^\infty {\rm d}t\, t\, f_\theta(t) \end{aligned} \tag{36}$$

where $\tau_{\rm r}$ is the absolute refractory period. The higher moments of the interspike interval distribution also play an important role in understanding the properties of the model. In particular, the coefficient of variation $C_{\rm V}$ of the interspike interval distribution,

$$C_{\rm V} = \frac{\sqrt{{\rm Var}[T_{\rm ISI}]}}{{\rm E}[T_{\rm ISI}]} = \frac{[\overline{(T_{\rm ISI} - \overline{T}_{\rm ISI})^2}]^{1/2}}{\overline{T}_{\rm ISI}}, \tag{37}$$

is an important measure of the variability of the neural response. For a homogeneous Poisson distribution, it has the value $C_{\rm V} = 1$. The variability of neuronal spiking and the role of the integrate-and-fire neuron model is discussed further in Sect. 7.1.

4.1 The perfect integrator neuron model

The solution for the perfect integrator neuron model with current synapses and homogeneous Poisson input in the case where there are only excitatory input follows straightforwardly from the Poisson statistics. If the threshold is reached with m_θ excitatory synaptic inputs (of uniform amplitude), then the output interspike interval distribution is exactly the distribution of the $m_\theta^{\rm th}$ input

$$f_{m_\theta}(t) = \frac{\lambda_{\rm E}^{m_\theta} t^{m_\theta - 1} {\rm e}^{-\lambda t}}{(m_\theta - 1)!}. \tag{38}$$

The solution of the spike output density for the homogeneous Poisson process with both excitatory and inhibitory inputs may be calculated using the renewal equation for the first passage time density, obtained using Laplace transforms (Tuckwell 1988b),

$$f_{m_\theta}(t) = m_\theta \left(\frac{\lambda_{\rm E}}{\lambda_{\rm I}}\right)^{m_\theta/2} \frac{{\rm e}^{-(\lambda_{\rm E}+\lambda_{\rm I})t}}{t} I_{m_\theta}(2t\sqrt{\lambda_{\rm E}\lambda_{\rm I}}), \tag{39}$$

where m_θ is the value of the threshold above the resting potential V_0 (in units of $a = a_{\rm E} = a_{\rm I}$) and I_m is the modified Bessel function.

A solution may also be obtained by approximating the random arrival times using a Wiener process (Gerstein and Mandelbrot 1964), as described in Sect. 3.1.1. The mean and variance of the process are

$$\begin{aligned} \mu(t; v_0) &= {\rm E}[v(t)|v_0, t_0 = 0] = v_0 + \mu_{\rm W} t, \\ \sigma^2(t; v_0) &= {\rm Var}[v(t)|v_0, t_0 = 0] = \sigma_{\rm W}^2 t. \end{aligned} \tag{40}$$

The drift, $\mu_{\rm W} > 0$, and variance parameter, $\sigma_{\rm W}^2$, for a neuron with current synapses (Sect. 2.1.1) and Poisson-distributed input described by Eq. (5) are given by

$$\mu_{\rm W} = a_{\rm E}\lambda_{\rm E} - a_{\rm I}\lambda_{\rm I}, \quad \sigma_{\rm W}^2 = a_{\rm E}^2\lambda_{\rm E} + a_{\rm I}^2\lambda_{\rm I}. \tag{41}$$

For positive drift, $\mu_{\rm W} > 0$, the probability of firing is 1, whereas for negative drift, $\mu_{\rm W} < 0$, inhibition is greater than excitation and the probability of firing is less than 1. It is possible to overcome this problem by imposing a reflecting boundary at some potential below v_0, and the properties of this model (incorporating a constant decay term) have been investigated using the Fokker–Planck equation (Fusi and Mattia 1999).

The solution for the output interspike interval distribution (the density of the first passage time), obtained using the renewal equation and Laplace transforms, is (Gerstein and Mandelbrot 1964; Tuckwell 1988b)

$$f_\theta(t) = \frac{\theta}{\sqrt{2\pi\sigma_{\rm W}^2 t^3}} \exp\left\{-\frac{(\theta - \mu_{\rm W} t)^2}{2\sigma_{\rm W}^2 t}\right\}. \tag{42}$$

This is an inverse Gaussian distribution (Chhikara and Folks 1989). The mean of the interspike interval distribution is $T_{\rm ISI} = \theta/\mu_{\rm W}$ and the variance is $\theta\sigma_{\rm W}^2/\mu_{\rm W}^3$, giving a coefficient of variation $C_{\rm V} = \sigma_{\rm W}/\sqrt{\theta\mu_{\rm W}}$. Recent investigations of the perfect integrator with colored noise have been carried out (Middleton et al. 2003; Lindner 2004).

4.2 The leaky integrate-and-fire neuron model

A number of authors have subsequently analyzed the leaky integrate-and-fire neuron model (Geisler and Goldberg 1966;

Roy and Smith 1969), including Gluss (1967), who obtained a solution to the first passage time problem in terms of an expression for its Laplace transform, from which it is straightforward to obtain expressions for all the moments of the distribution. The moments of the first passage time distribution were first derived by Johannesma (1968) Siebert (1969) was the first to explicitly derive the first passage time density. Sugiyama et al. (1970) provided an alternative solution using a Laplace transform approach, which they compared with the numerical results of finite-difference equations. A derivation of the first passage time distribution was also given by Capocelli and Ricciardi (1971).

For the leaky integrate-and-fire neuron model with current synapses and homogeneous Poisson δ-function inputs, Eqs. (4) and (5), the conditional mean and variance of the free membrane potential are given by Eqs. (20) and (21). The parameters ($\mu_{\rm Q}$, $\sigma_{\rm Q}^2$, $\tau_{\rm m}$) are identified as (μ, σ^2, τ) respectively, in the Ornstein–Uhlenbeck Eq. (15).

The output spiking-rate is given by

$$\lambda_{\rm out} = \left\{ \tau_{\rm r} + \frac{\tau_{\rm Q}}{\sigma_{\rm Q}} \sqrt{\frac{\pi}{2}} \int_{V_{\rm reset}}^{V_{\rm th}} {\rm d}u \exp\left[\frac{(u-\mu_{\rm Q})^2}{2\sigma_{\rm Q}^2} \right] \times \left[1 + {\rm erf}\left(\frac{u-\mu_{\rm Q}}{\sigma_{\rm Q}\sqrt{2}} \right) \right] \right\}^{-1} \tag{43}$$

where erf is the error function. For the leaky integrate-and-fire neuron model with current synapses and δ-function inputs the membrane time constant is the passive time constant, $\tau_{\rm Q} = \tau_{\rm m}$. This is the so-called Siegert formula (Siegert 1951; Ricciardi 1977; Tuckwell 1988b; Amit and Tsodyks 1991). For details of a derivation using the Gaussian approximation and a Laplace transform approach based upon the renewal equation, Eq. (24), which requires careful consideration of the finite and divergent parts of the resultant integrals, see (Burkitt et al. 2003, App. A). For details of a derivation using the Fokker–Planck equation, see Brunel and Hakim (1999). Note that once the parameters $V_{\rm th}$ and $V_{\rm reset}$ have been chosen, this formula gives the mean spiking-rate as a function of the three variables $\mu_{\rm Q}$, $\sigma_{\rm Q}$, and $\tau_{\rm Q}$, which are experimentally accessible (Inoue et al. 1995; Destexhe and Paré 1999). The case of current inputs with a finite synaptic time constant is discussed in Sect. 5.1.

The stationary distribution of the membrane potential, $P_0(v)$, for the model with current synapses is (Brunel and Hakim 1999)

$$P_0(v) = \frac{\lambda_{\rm out}\tau_{\rm Q}}{\sigma_{\rm Q}} \exp\left[\frac{(v-\mu_{\rm Q})^2}{2\sigma_{\rm Q}^2} \right] \times \int_{v}^{V_{\rm th}} {\rm d}u \exp\left[\frac{(u-\mu_{\rm Q})^2}{2\sigma_{\rm Q}^2} \right] \Theta(u - V_{\rm reset}), \tag{44}$$

where $\Theta(x)$ is the Heaviside step function.

The analysis for the case with conductance synapses is not so straightforward, since the corresponding Stein model, Eq. (23), has voltage-dependent jumps in the membrane potential. Early studies of this model with conductance synapses typically approximated the first passage time by the instant at which the mean membrane potential crosses the threshold. This procedure breaks down when the mean membrane potential asymptotically approaches a sub-threshold value.

It is, however, possible to find an analytic solution for δ-function conductance synaptic input using the Stein model (Hanson and Tuckwell 1983), or the Gaussian approximation (Burkitt 2001), and the values of $\mu_{\rm Q}$, $\sigma_{\rm Q}^2$, and $\tau_{\rm Q}$ are

$$\begin{aligned} \mu_{\rm Q} &= \tau_{\rm Q}\left(\frac{V_0}{\tau_{\rm m}} + r_{11} \right) \\ \sigma_{\rm Q}^2 &= \frac{\mu_{\rm Q}^2 r_{20} - 2\mu_{\rm Q} r_{21} + r_{22}}{2/\tau_{\rm Q} - r_{20}} \end{aligned} \tag{45}$$

$$\begin{aligned} \tfrac{1}{\tau_{\rm Q}} &= \frac{1}{\tau_{\rm m}} + r_{10} \\ r_{kl} &:= \lambda_{\rm I} g_{\rm I}^k V_{\rm I}^l + \lambda_{\rm E} g_{\rm E}^k V_{\rm E}^l, \end{aligned} \tag{46}$$

where $(kl) = \{(10), (11), (20), (21), (22)\}$. Introducing the total excitatory and inhibitory conductances

$$G_{\rm E} = g_{\rm E}\lambda_{\rm E}, \quad G_{\rm I} = g_{\rm I}\lambda_{\rm I}, \tag{47}$$

the expressions for the equilibrium value of the membrane potential and the effective membrane time constant take the simple form

$$\begin{aligned} \frac{1}{\tau_{\rm Q}} &= g_{\rm L} + G_{\rm E} + G_{\rm I} \\ \mu_{\rm Q} &= \tau_{\rm Q}\left(g_{\rm L} V_0 + G_{\rm E} E_{\rm E} + G_{\rm I} E_{\rm I} \right), \end{aligned} \tag{48}$$

where $g_{\rm L}$ is the passive leakage conductance. As before, the parameter $\mu_{\rm Q}$ represents the average equilibrium value of the membrane potential in the absence of spike generation. The membrane potential decays with time, displaying leakage with time constant $\tau_{\rm Q}$.

In the large $N_{\rm E}$, $N_{\rm I}$ limit, the individual synaptic conductances (somewhat surprisingly) do not scale – it is sufficient that $g_{\rm E}$, $g_{\rm I} << 1$. This is due to the increased leakage in the model with conductance synapses, and it is in contrast to the case with current synapses, for which $a_{\rm E}$, $a_{\rm I}$ scale as $1/\sqrt{N}$, with $N = N_{\rm E}$, $N_{\rm I}$, respectively.

The resulting output spiking-rate is given by Eq. (43) with the values of $\mu_{\rm Q}$, $\sigma_{\rm Q}^2$, and $\tau_{\rm Q}$ given above (Burkitt 2001). A similar expression have been arrived at using a Fokker–Planck formalism (Richardson 2004)

$$\lambda_{\rm out} = \left[\tau_{\rm r} + 2 \int_{V_{\rm reset}}^{V_{\rm th}} {\rm d}u {\rm e}^{-K(u)} \int_{-\infty}^{u} {\rm d}x \frac{{\rm e}^{K(x)}}{B(x)} \right]^{-1}, \tag{49}$$

where for homogeneous synaptic input both the drift and diffusion functions, $A(v)$ and $B(v)$ in Eq. (34), are independent of time and

$$K(v) = -\frac{1}{\tau_Q r_{20}} \ln\left(r_{20}v^2 - 2r_{21}v + r_{22}\right) + \left(2r_{11} - \frac{2r_{21}}{\tau_Q r_{20}}\right)\frac{1}{s_0}\arctan\left(\frac{2r_{20}v - 2r_{21}}{2s_0}\right)$$

$$s_0 = g_E g_I \sqrt{\lambda_E \lambda_I}(V_E - V_I). \tag{50}$$

The two expressions for the spiking-rate with conductance synapses, Eqs. (43) and (49), agree in the regime where the diffusion approximation is good.

The stationary distribution of the membrane potential, $P_0(v)$, for the model with conductance synapses and homogeneous synaptic input is (Richardson 2004)

$$P_0(v) = \frac{2\lambda_{out}}{B(v)} e^{K(v)} \int_v^{V_{th}} du e^{-K(u)} \Theta(u - V_{reset}). \tag{51}$$

The essential difference of conductance synapses to current synapses is that the membrane potential approaches μ_Q with an *effective* membrane time constant τ_Q that is less than the passive membrane time constant τ_m because of the effect of the synaptic conductances, as originally recognized by (Johannesma 1968). It is apparent from these equations that as the input rates λ_E and λ_I increase, the effective time constant τ_Q decreases, due to the neuron becoming more leaky as more synaptic channels open (Tiesinga et al. 2000). The case of conductance synaptic inputs with a finite synaptic time constant is discussed in Sect. 5.1 and a more detailed discussion of the issues associated with conductance synapses is given in (Richardson and Gerstner 2005).

5 Extensions of the integrate-and-fire neuron model

5.1 Finite synaptic time constants

The effect of the synaptic time constant τ_s may be approximated in the model by modeling the synaptic input as a dynamical quantity. In the case of current synapses, the membrane voltage is given by

$$\tau_m \frac{dv(t)}{dt} = -[v(t) - V_0] + R_m I_s(t), \tag{52}$$

and the synaptic current $I_s(t)$ obeys the Langevin equation

$$\tau_s \frac{dI_s(t)}{dt} = -I_s(t) + \mu + \sigma\sqrt{2\tau_s}\xi(t), \tag{53}$$

where $\xi(t)$ is Gaussian white noise and μ, σ are the mean and variance of the input synaptic current, given by Eq. (21). The synaptic current consequently has an exponential correlation with time constant τ_s. It is then possible to write a Fokker–Planck equation for the probability density $P(v, I_s, t)$ (Brunel and Sergi 1998). The stationary solution can be approximated by expanding as a power series in the parameter $k = \sqrt{\tau_s/\tau_m} < 1$. The output spiking-rate to first order in k is given by (Brunel and Sergi 1998; Fourcaud and Brunel 2002).

$$\lambda_{out} = \left\{\tau_r + \frac{\tau_Q}{\sigma_Q}\sqrt{\frac{\pi}{2}} \int_{V_{reset}+k\alpha\sigma_Q}^{V_{th}+k\alpha\sigma_Q} du \exp\left[\frac{(u-\mu_Q)^2}{2\sigma_Q^2}\right] \times \left[1 + \mathrm{erf}\left(\frac{u-\mu_Q}{\sigma_Q\sqrt{2}}\right)\right]\right\}^{-1}, \tag{54}$$

where $\alpha = |\zeta(1/2)|$ and ζ is the Riemann zeta function. The approximation to the stationary distribution of the membrane potential, $P_0(v)$, is likewise obtained by adding the correction term $k\alpha\sigma_Q$ to both V_{reset} and V_{th} in the expression for $P_0(v)$ in Eq. (44). This method has also been used for studying the leaky integrate-and-fire neuron model with current synapses and oscillatory input current (Fourcaud and Brunel 2002). An expansion in the parameter $\sqrt{\tau_m/\tau_s} < 1$ for large synaptic time constants, also using the Fokker–Planck formalism, is given by (Moreno-Bote and Parga 2004).

In the case of conductance synapses, finite synaptic time constants are introduced in an analogous fashion to current synapses, Eq. (53), by modeling the conductances as a Langevin equation

$$\tau_s \frac{dg(t)}{dt} = -g(t) + g_0 + \sigma_g\sqrt{2\tau_s}\xi(t), \tag{55}$$

where $\xi(t)$ is Gaussian white noise, g_0 and σ_g are the mean and variance of the conductance fluctuations, and in general there are different synaptic time constants associated with each type (E, I) of conductance in the model. This model has been investigated using numerical simulations (Destexhe et al. 2001). The analytical study of this model is somewhat more complicated than for current synapses, since the resulting fluctuations are not simply additive (as they are for current synapses) but have a component with a multiplicative dependence upon the membrane potential, as described in Eq. (10). A perturbation method has been developed (Richardson and Gerstner 2005) that successfully describes the non-Gaussian nature of the free membrane potential distribution, giving the effective-time-constant approximation (Burkitt 2001) to leading order while the higher orders give the skew of the distribution. However, this multiplicative noise means that there is no straightforward extension of the results for the spiking-rate and C_V obtained for δ-function conductance synaptic input using the Fokker–Planck formalism (Lindner and Longtin 2005a, in press).

5.2 Temporal correlations in the synaptic input

The existence of correlations in the arrival times of input on different synapses has been postulated as a cause of the observed variability of output spike times (Stevens and Zador 1998). Such temporal correlations in the synaptic input current $I_s(t)$ can be included by modeling the current as colored noise, $\eta(t)$,

$$\langle\eta(t)\rangle = 0, \quad \langle\eta(t)\eta(t')\rangle = \exp\left(\frac{-|t-t'|}{\tau_c}\right), \tag{56}$$

where τ_c is the time constant of the input correlations (in the limit $\tau_c \to 0$, $\eta(t)$ becomes a Gaussian random variable). Colored noise can be generated from Gaussian white noise using the Langevin equation

$$\tau_c \frac{d\eta(t)}{dt} = -\eta(t) + \sqrt{2\tau_c}\xi(t), \tag{57}$$

where $\xi(t)$ is Gaussian noise. This introduces a filtering of the same type as that considered above in relation to finite synaptic time constants, and the same methods have been employed to study temporal correlations, both with numerical simulations (Sakai et al. 1999) and the Fokker–Planck approach (Moreno et al. 2002). The impact of temporal correlations in the synaptic input upon the variability of output spike times has subsequently been examined by a number of authors both analytically in the perfect integrator (Salinas and Sejnowski 2000; Feng and Brown 2000) and numerically in the leaky integrate-and-fire neuron model, with binary valued current synapses (Salinas and Sejnowski 2002) and with conductance synapses (Salinas and Sejnowski 2000; Svirskis and Rinzel 2000; Feng and Brown 2000; Stroeve and Gielen 2001). The results indicate that such temporal correlations increase the variability, as well as playing a role in regulating the gain of the output spiking-rate. A discussion of other possible sources of spike timing variability is given in Sect. 7.1 and of gain modulation in Sect. 7.2. In addition to pairwise correlations of the sort discussed above, it has also been found that the higher-order statistics can have an effect upon the firing rate of neurons (Kuhn et al. 2003).

5.3 Adaptation and relative refractory effects

Spike-rate adaptation is the observed lengthening of the interspike intervals over time when a neuron is injected with a constant current, before it settles into a steady-state value. The inclusion of adaptation into the framework of integrate-and-fire neuron models is problematic, since the reset mechanism after the generation of an output spike in the integrate-and-fire neuron model means that both the past spike times and the previous time course of the membrane potential are forgotten. This renewal behavior is what facilitates the analytic study of integrate-and-fire neuron models, but makes including adaptation effects difficult.

In order to include adaptation effects in the leaky integrate-and-fire neuron model with conductance synapses, an adaptation current is introduced (Wehmeier et al. 1989; Salinas and Sejnowski 2000)

$$I_{\text{adapt}}(t) = -g_{\text{adapt}}(t)[v(t) - V_0], \tag{58}$$

where $g_{\text{adapt}}(t)$ is a time-dependent shunting conductance with an associated reversal potential equal to the resting potential. Each output spike increases this conductance by a fixed amount g_{inc} and between spikes the conductance decays with an associated time constant, τ_{adapt},

$$\tau_{\text{adapt}}(t) \frac{dg_{\text{adapt}}(t)}{dt} = -g_{\text{adapt}}(t) + \sum_{\{t_{\text{out}}\}} g_{\text{inc}} \delta(t - t_{\text{out}}), \tag{59}$$

where $\{t_{\text{out}}\}$ are the output spike times. The rationale is that this adaptation mechanism mimics the activation of the fast potassium current that occurs after a spike is generated (McCormick et al. 1985). This current is not reset when an output spike is generated and consequently it contains information about the past spiking behavior of the neuron.

An extensive study of spike-rate adaptation and its role in the temporal properties of neuronal computation has been carried out (Liu and Wang 2001), using a leaky integrate-and-fire model with a Ca^{2+}-activated K^+ current (Wang 1998). They find an analytic expression for the adaptation time constant τ_{adapt} in terms of the Ca^{2+} decay time constant and other neural parameters, and explore the variability of the interspike intervals. Similar results are obtained using a more general approach to adaptation (i.e., not tied to the Ca^{2+}-dependent K^+ channel) and also showed that adaptation linearizes the input-output curve for constant current injection, namely the singularity of the slope at the spiking threshold becomes finite [cf. discussion following Eq. (14)] (Ermentrout 1998; Benda and Herz 2003). A similar model of spike adaptation has been used in a study of contrast invariance of neurons in the visual cortex (Hansel and van Vreeswijk 2002), in neocortical rhythms (Fuhrmann et al. 2002), and in the response of neurons to in vivo-like currents (Rauch et al. 2003).

A number of alternative methods to introduce spike-rate adaptation have been proposed. One method is to increase the threshold for a time following the generation of a spike, and a review of early work using models of this type is given by (Holden 1976, Chap. 4.4). Such a transient increase of the threshold following a spike has also been used as a technique to include a relative refractory period into the model (Tuckwell 1978b; Wilbur and Rinzel 1983; Tuckwell and Wan 1984). The model displays the progressive decrease in the spiking-rate following the onset of a stimulus that characterizes adaptation, as well as a correlation of the interspike intervals (Chacron et al. 2003). Analytical expressions for the mean and variance of the interspike interval have been found for the case where the modification to the threshold is small (Lindner and Longtin 2005b). Another method for modeling refractoriness is to consider the spiking threshold as an elastic barrier (Buonocore et al. 2002).

Wilbur and Rinzel (1983) carried out a numerical investigation of the leaky integrate-and-fire neuron model with conductance synapses using a time-varying spiking threshold. They used both Monte Carlo simulations and numerical methods for solving partial differential equations to show that a time-dependent threshold is capable of producing results that more closely agree with experimental data. Moreover, such a time-dependent threshold is equivalent to allowing a partial reset of the membrane potential following each spike (Bugmann et al. 1997).

The effect of noise adaptation, namely how a step increase in the root-mean-square level of input noise produces a transient increase in the spiking-rate of integrate-and-fire neurons, is discussed in (Rudd and Brown 1997).

Recent studies have employed the population density approach to investigate both of the above mechanisms of adaptation (adaptation current and time-dependent threshold) to examine the time-varying behavior of a large population of adapting integrate-and-fire neurons with conductance synapses (La Camera et al. 2004).

6 Relationship to the Hodgkin–Huxley model and electrophysiological data

6.1 Hodgkin–Huxley model

The Hodgkin–Huxley model of the membrane potential is the classic description of both the subthreshold behavior and the spiking behavior of the membrane potential (Hodgkin and Huxley 1952). It is an equation of the form given in Eq. (1), but with a spiking current I_{spike} [cf. Eq. (3)]

$$I_{\text{spike}}(t) = g_{\text{Na}} m^3 h(v(t) - V_{\text{Na}}) + g_{\text{K}} n^4 (v(t) - V_{\text{K}}), \quad (60)$$

where g_{Na} and g_{K} are the sodium and potassium conductances, respectively, V_{Na} and V_{K} are their associated reversal potentials, m and n are the sodium and potassium activation variables, and h is the sodium inactivation variable. The voltage dependence of the variables m, h, and n provides a description of the time course of an action potential.

The relationship between the Hodgkin–Huxley model and other neuron models has been examined by a number of authors (Abbott and Kepler 1990). The standard leaky integrate-and-fire neuron model can*not* be derived from conductance-based models such as the Hodgkin–Huxley model using a rigorous reduction procedure. However, it is possible to approximate the Hodgkin–Huxley model by a response kernel expansion in terms of a single variable describing the membrane voltage. The truncation of this expansion beyond the first-order kernel has been shown to be equivalent to a form of the leaky integrate-and-fire neuron model (Kistler et al. 1997), namely the spike response model (Gerstner 1995). Numerical comparisons of this threshold model with the Hodgkin–Huxley model with stochastic input current have shown that the threshold model provides a good approximation that justifies the threshold description of the spiking behavior. The relationship between the Hodgkin–Huxley model and the leaky integrate-and-fire model, as well as a pulse-based model, is examined in detail in (Destexhe 1997).

6.2 Comparison of integrate-and-fire neurons with electrophysiological data

There are three classes of parameters that characterize the integrate-and-fire neuron model. First, there are the intrinsic parameters characterizing the neuron, such as the firing threshold V_{th}, the resting potential V_0, the reset potential following a spike V_{reset} (often taken in the model to be equal to the resting potential), the reversal potentials V_{E}, V_{I}, and the passive membrane time constant τ_{m}. These parameters are not dependent upon the activity of the neuron (i.e., the response to synaptic input) and can be determined by direct methods (i.e., observing responses to injected current). There are well-established methods for determining these parameters (Tabak et al. 2000) and they will not be discussed further here. Second, the parameters associated with the response of the membrane potential to stochastic synaptic input, namely the three variables μ_{Q}, σ_{Q}, and τ_{Q}. These parameters are experimentally accessible from intracellular recordings. Third, the parameters associated with the input to the neuron, namely the amplitudes a_{E}, a_{I} (or g_{E}, g_{I} for models with conductance synapses), spiking-rate λ_{E}, λ_{I}, and the number of synaptic inputs N_{E}, N_{I}. These parameters are usually not directly experimentally accessible and must be deduced from the observed activity, either intracellularly or extracellularly. When considering in vivo data, the second set of parameters (associated with the membrane potential) are clearly intimately related to the third set (associated with the input to the model).

There has been comparatively little work done on the systematic estimation of these parameters from electrophysiological data. A proper estimation of the parameters enables a systematic comparison of the model with the data using statistical techniques and is an important step in the validation of the model. Early work comparing the model with experimental data centered around a comparison of extracellular recordings (i.e., the moments of the interspike interval distribution) with model parameters. Fits of the interval histogram data to the inverse Gaussian distribution, Eq. (42), for the perfect integrator (Gerstein and Mandelbrot 1964), were obtained using both least-squares and maximum likelihood estimation methods (Nilsson 1977). A comparison of the first three moments of the diffusion approximation of the leaky integrate-and-fire neuron model with experimental data enabled the number of synaptic inputs to the neuron to be estimated (Tuckwell and Richter 1978). The difficulty of these estimation techniques is that they are based upon complex analytical expressions for the moments of the interspike interval distributions. In order to overcome this difficulty, maximum likelihood estimation methods were proposed for the comparison of mean μ and variance σ of the membrane potential with recordings of the intracellular trace between consecutive spikes (Brillinger and Segundo 1979; Lánský 1983). Subsequent neural parameter estimator studies have elaborated these two methods, followed either methods based on extracellular data (O'Neill et al. 1986; Lánský and Radil 1987; Brillinger 1988; Inoue et al. 1995; Paninski et al. 2004) or intracellular data (Habib and Thavaneswaran 1990; Lánská and Lánský 1998). Recent studies have made use of large-scale numerical simulations (Destexhe and Paré 1999) and whole-cell recordings using the dynamic-clamp technique, in which the response of a neuron to an injected stochastic current with parameters (μ, σ) is observed (Destexhe et al. 2001). Rather than using analytical fitting techniques, some studies have implemented Monte Carlo parameter estimation techniques (Rauch et al. 2003). Parameter estimation

using the dynamic-clamp technique has been extended to take account of network behavior (Giugliano et al. 2004).

7 Discussion

The integrate-and-fire neuron model has proven useful in addressing many of the questions about how neurons and neural systems process information. The sheer quantity of such investigations means that a review such as this must be somewhat selective, both in terms of the issues addressed and the papers cited. In particular, it is not possible to review the many applications of the integrate-and-fire neuron model that are modality specific, i.e., that address-specific questions in the visual, auditory, olfactory, somatosensory, or motor systems. The questions addressed below have been chosen to illustrate how the model has played, and is playing, an important role in elucidating some of the broader key issues in our understanding of neural systems.

7.1 ISI variability with the integrate-and-fire neuron model

The irregular firing of cortical neurons in vivo has frequently been used to make inferences about the cortical code and cortical processing. A measure of this irregularity is the coefficient of variation of the interspike intervals, given in Eq. (37). Softky and Koch (1992, 1993) pointed out that the integration of many randomly arriving excitatory postsynaptic potentials leads to highly regular, rather than irregular, neural firing. Experimental evidence (Bryant and Segundo 1976; Mainen and Sejnowski 1995) suggests that the spiking mechanism is very reliable, and so the synaptic input must be correlated, causing irregular fluctuations in the membrane potential, or there must be some strong dendritic nonlinearities in neural processing. Subsequent studies showed that highly irregular spiking can also result from either a short membrane time constant (i.e., the neuron behaves as a coincidence detector, responding to random variations in the membrane potential), or from a balance between excitation and inhibition, which can cause the membrane potential to have an equilibrium value just below threshold, so that random small fluctuations can generate spikes (Shadlen and Newsome 1994, 1998). Moreover, such an approximate balance of excitation and inhibition produces an effective membrane time constant that is much shorter than the passive membrane time constant, as discussed in Sect. 4.2, and is therefore a likely cause of the irregular firing.

It is beyond the scope of this review to give a full description of the extensive research and the numerous mechanisms that have been proposed as an explanation of the observed irregular spiking in cortical neurons. However, the integrate-and-fire neuron model has played an important role in uncovering some of the important issues associated with irregular spiking behavior, and some of the papers that have used the model are discussed here briefly. One of the earliest analyses of the coefficient of variation using the integrate-and-fire neuron model with conductance synapses (Tuckwell 1979) showed that a large amount of inhibition could produce a value of C_V greater than 1. This result was subsequently disputed in a study that showed that such large values of C_V within a physiologically realistic parameter range required the introduction of a time-varying (decaying) threshold to model refractory effects (Wilbur and Rinzel 1983). There have been a number of more recent investigations of the effect of an exponentially decaying threshold on the ISI variability (Chacron et al. 2003; Lindner and Longtin 2005b), which introduces correlations between successive interspike intervals as discussed in relation to adaptation (Sect. 5.3).

There are a number of other factors that can have an effect upon the temporal structure of the output spike times. Correlations within the synaptic input have been implicated as a source of the high ISI variability observed, and such correlations can arise either through explicit temporal correlations between inputs on different synapses, as described in Sect. 5.2, or through finite synaptic time constants, as described in Sect. 5.1. The studies of the integrate-and-fire neuron model with temporal correlations discussed in these sections have shown that correlations can substantially increase the variability of the output spike times. Another proposed source of temporal correlations is through the spatial properties of the model neuron, namely taking into account the spatial extent of the dendritic tree (Kohn 1989). This is typically done by considering a two-compartment model, in which one compartment corresponds to the effect of the dendritic tree and the other to the spike initiation site (Lánský and Rospars 1995). The dendritic compartment is modeled using a diffusion process that is independent of the output spikes, whereas the spike initiation compartment is modeled as a simplified RC-circuit. The output spikes generated in this model have been found to be temporally correlated (Lánský and Rodriguez 1999a,b). Another effect upon the temporal structure of the output spike times is the possibility of a randomized distribution of reset potentials following the generation of a spike (Lánský and Musila 1991). Introducing such a random reset value of the membrane potential causes an increase in the variability of the output spikes (Lánský and Smith 1989). The effect upon C_V of a partial reset of the membrane potential was investigated by (Troyer and Miller 1997) and was further examined in considerable detail by (Bugmann et al. 1997), where it was shown to be equivalent to the use of a time-dependent threshold, as described above.

While most models consider Poisson-distributed synaptic inputs, some analyses of real spike data shows that it can exhibit long-range dependence, and this can have a significant influence upon the variability of the output spikes (Jackson 2004). An analysis of the effect of such long-range dependence upon the spiking-rate and C_V has been carried out in the perfect integrator (Middleton et al. 2003) and the leaky integrate-and-fire neuron model (Jackson 2004).

Other mechanisms that address the question of output spike variability include the interaction of random synaptic

input with nonlinearities in type I Hodgkin–Huxley spike dynamics (Gutkin and Ermentrout 1998).

The observed spike time variability may also arise through network mechanisms, such as the amplification of correlated fluctuations in a recurrent network. This mechanism has been shown to give high values of C_V in a numerical study of a network of leaky integrate-and-fire neurons (Usher et al. 1994). A comparison of the C_V between two analytical studies of a sparsely connected network of integrate-and-fire neurons, one with current synapses (Brunel 2000) and the other with conductance synapses (Meffin et al. 2004), indicates that different mechanisms underlie the irregular spiking in these two models. In the case of conductance-based synapses, irregular firing is maintained across different levels of external input through changes in the effective membrane time constant τ_Q (Meffin et al. 2004). This causes a rapid charging of the membrane potential to values just below threshold, and random fluctuations then occasionally cause it to cross threshold. This mechanism does not require a strict balance between excitation and inhibition, which *is* required in the case of current synapses. Similar conclusions were reached in a simulation based study (Rudolph and Destexhe 2003).

7.2 Gain modulation

Gain modulation describes how the amplitude of the output response of a system can be changed in a nonlinear way, in particular how a neuron's spiking-rate (in response to a stimulus) is modulated by other features in the external or internal environment. This allows information to be transformed, combined or compared, and consequently gain modulation provides an important means by which an organism can respond appropriately to its environment. Physiological studies have observed gain modulation both in many neural functions and in a number of brain areas, but the underlying mechanisms are not well understood. The central question concerning gain modulation is how neurons achieve the nonlinear, multiplicative behavior characteristic of gain modulation when their input–output relationship is basically integrative. A number of possible mechanisms have been proposed for neural gain modulation at the single neuron level, as reviewed by (Salinas and Thier 2000). One approach involves the effect of correlated synaptic input (see Sect. 5.2), in which an analysis of an integrate-and-fire neural model indicates that the gain can be modulated by the degree of correlation of the synaptic inputs (Salinas and Sejnowski 2000).

Another approach involves the effect of the balanced component of the synaptic input in providing the nonlinear gain modulation of the neural response to an additional *driving* synaptic input (Chance et al. 2002). An analysis of gain modulation using the leaky integrate-and-fire neural model with conductance synapses showed that the effect of increasing the balanced background activity can be understood in terms of two competing processes, both influenced by the effective membrane time constant, τ_Q (Burkitt et al. 2003). First, the contribution of a driving excitatory synaptic input to the mean membrane potential is approximately linear in the spiking-rate of the driving input. As the level of background activity increases, the effective time constant, τ_Q, decreases, resulting in a lower value of μ_Q for a given driving spiking-rate [see Eq. (45)]. This decrease in τ_Q is due to the neuron becoming more leaky as more synaptic channels open (Tiesinga et al. 2000). The value of σ_Q remains approximately constant for all conditions and driving spiking-rates, also as a result of the increased leakiness. Although lower values of μ_Q are expected to decrease the output spiking-rate, this is offset by a second effect: the neuron operates on a faster time scale as τ_Q decreases, and so the time course and fluctuations in the membrane potential are more rapid. When the neuron is in the linear input–output regime these two competing effects approximately cancel and there is no gain modulation. When the neuron is in the nonlinear regime the effect of the extra leakiness dominates over the effect of the faster time scale, resulting in diminished gain as the level of background activity increases (Meffin et al. 2005). Similar conclusions were reached in related studies (Murphy and Miller 2003; Yu and Lee 2003; Kuhn et al. 2004).

The conditions that characterize the linear and nonlinear behavior can be understood by reparameterizing the output spiking-rate, Eq. (43), as (Burkitt et al. 2003)

$$\begin{aligned}\lambda_{\text{out}} &= \frac{1}{\tau_Q} F\left(\frac{\mu_Q - V_{\text{th}}}{\sqrt{2}\sigma_Q}; \frac{\sigma_Q}{\theta}\right) \\ &= \frac{1}{\tau_Q}\left[\int_{-\frac{(\mu_Q - V_{\text{th}})}{\sqrt{2}\sigma_Q} - \frac{\theta}{\sqrt{2}\sigma_Q}}^{-\frac{(\mu_Q - V_{\text{th}})}{\sqrt{2}\sigma_Q}} \mathrm{d}u \sqrt{\pi} \mathrm{e}^{u^2} (1 + \operatorname{erf} u)\right]^{-1},\end{aligned} \tag{61}$$

where the absolute refractory period term has been neglected, since we are interested in comparatively low spiking-rates where it plays little role. Figure 4 shows that the function F is approximately linear in the first argument, $x = (\mu_Q - V_{\text{th}})/\sqrt{2}\sigma_Q$, for moderate and large values of x. Two important implications follow from this result (Burkitt et al. 2003). First, a linear input–output curve can result even when μ_Q is less than threshold. Second, the transition from linear to nonlinear behavior occurs when the output spiking-rate becomes sufficiently large, as illustrated in Fig. 4b. This provides a second criterion for the presence of gain modulation behavior that relates directly to the output spiking-rate.

Other mechanisms for gain control using the integrate-and-fire neuron model with conductance synapses have been investigated by a number of authors, including the study of the effect of neuromodulators acting postsynaptically, inhibitory feedback and presynaptic inhibition (Capaday 2002), and studies of shunting inhibition (Doiron et al. 2000; Longtin et al. 2002).

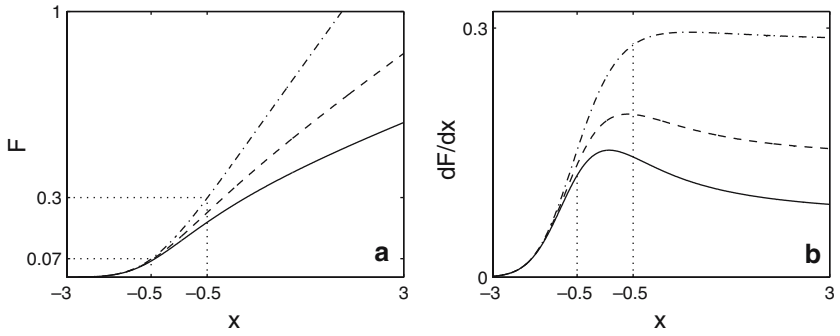

Fig. 4 Illustration of gain modulation in the integrate-and-fire neuron model. **a** The function F, Eq. (61), and **b** its derivative with respect to its first argument $x = (\mu_Q - V_{th})/\sqrt{2}\sigma_Q$ for several values of its second argument $\sigma_Q/\theta = 0.05$ (*solid*), 0.1 (*dashed*) and 0.2 (*dot-dashed*). The *vertical dotted lines* in (**b**) illustrate the region $-1.5 \leq x \leq -0.5$ in which a transition from nonlinearity to linearity occurs, depending on the values of σ_Q/θ and the strictness of the criteria for linearity. The *dotted lines* in (**a**) give the corresponding region and values of the function F. (Taken from Burkitt et al. 2003)

8 Conclusions

The integrate-and-fire neuron model has been a very useful tool in the quest to understand how neural systems function and how they process information. The separation of the time scales in the model between the relatively slow subthreshold integration of synaptic inputs and the rapid spike generation has captured a significant part of the essential character of neural processing. The model is sufficiently simple to provide both analytical methods of solution and intuitive insights into a number of important questions.

However, the model also has a number of shortcomings associated with the simplifying assumptions that form part of the model, such as the neglect of the spiking mechanisms and the lack of spatial structure. The model represents a balance between conceptual simplicity and biological accuracy. The perfect integrator with current synapses, for example, is relatively straightforward to analyze, but the results can be used as a guide to actual neural behavior only in limited situations. The various extensions to the model to include more biological features, as discussed in Sect. 5, extend the applicability of the model but lead to increasing complexity in the mathematical analysis of the model.

Nevertheless, the advantages possessed by the integrate-and-fire neuron model mean that, despite these shortcomings, it will very likely continue to play an active role in our understanding of neural information processing, particularly in those areas in which the network dynamics (as opposed to the single neuron properties) is crucial to understanding the function of the neural system. These include an understanding of the control mechanisms and the control hierarchy in the brain, including the role of feedback (Laing and Longtin 2003) and network stability which are the subjects of a separate review (Burkitt 2006).

Acknowledgements The author thanks Hamish Meffin and David Grayden for a critical reading of the manuscript and detailed comments. This work was funded by the Australian Research Council (ARC Discovery Project #DP0453205), The Bionic Ear Institute, the LEW Carty Foundation, and the Jack Brockhoff Foundation.

References

Abbott LF, Kepler TB (1990) Model neurons: from Hodgkin–Huxley to Hopfield. In: Garrido L (ed) Statistical mechanics of neural networks. Springer, Berlin Heidelberg New York, pp 5–18

Amit DJ, Tsodyks MV (1991) Quantitative study of attractor neural network retrieving at low spike rates: I. Substrate–spikes, rates and neuronal gain. Netw Comput Neural Syst 2:259–273

Benda J, Herz AVM (2003) A universal model for spike-frequency adaptation. Neural Comput 15:2523–2564

Brillinger DR (1988) Maximum likelihood analysis of spike trains of interacting nerve cells. Biol Cybern 59:189–200

Brillinger DR, Segundo JP (1979) Empirical examination of the threshold model of neuron firing. Biol Cybern 35:213–220

Brunel N (2000) Dynamics of sparsely connected networks of excitatory and inhibitory spiking neurons. J Comput Neurosci 8:183–208

Brunel N, Hakim V (1999) Fast global oscillations in networks of integrate-and-fire neurons with low firing rates. Neural Comput 11: 1621–1671

Brunel N, Latham PE (2003) Firing rate of the noisy quadratic integrate-and-fire neuron. Neural Comput 15:2281–2306

Brunel N, Sergi S (1998) Firing frequency of leaky integrate-and-fire neurons with synaptic current dynamics. J Theor Biol 11:87–95

Brunel N, Hakim V, Richardson MJE (2003) Firing-rate resonance in a generalized integrate-and-fire neuron with subthreshold resonance. Phys Rev E 67:051916

Bryant HL, Segundo JP (1976) Spike initiation by transmembrane current: a white-noise analysis. J Physiol 260:279–314

Bugmann G, Christodoulou C, Taylor JG (1997) Role of temporal integration and fluctuation detection in the highly irregular firing of a leaky integrator neuron model with partial reset. Neural Comput 9:985–1000

Buonocore DV, Giorno V, Nobile AG, Ricciardi LM (2002) A neuronal modeling paradigm in the presence of refractoriness. BioSystems 67:35–43

Burkitt AN (2001) Balanced neurons: analysis of leaky integrate-and-fire neurons with reversal potentials. Biol Cybern 85:247–255

Burkitt AN (2006) A review of the integrate-and-fire neuron model. II. Inhomogeneous synaptic input and network properties. Biol Cybern (in press)

Burkitt AN, Clark GM (1999) Analysis of integrate-and-fire neurons: synchronization of synaptic input and spike output in neural systems. Neural Comput 11:871–901

Burkitt AN, Clark GM (2000) Calculation of interspike intervals for integrate-and-fire neurons with Poisson distribution of synaptic inputs. Neural Comput 12:1789–1820

Burkitt AN, van Hemmen JL (2003) How synapses in the auditory system wax and wane: theoretical perspectives. Biol Cybern 89:318–332

Burkitt AN, Meffin H, Grayden DB (2003) Study of neuronal gain in a conductance-based leaky integrate-and-fire neuron model with balanced excitatory and inhibitory synaptic input. Biol Cybern 89: 119–125

Calvin W, Stevens CF (1968) Synaptic noise and other sources of randomness in motoneuron interspike intervals. J Neurophysiol 31: 574–587

Capaday C (2002) A re-examination of the possibility of controlling the firing rate gain of neurons by balancing excitatory and inhibitory conductances. Exp Brain Res 143:67–77

Capocelli RM, Ricciardi LM (1971) Diffusion approximation and first passage time problem for a model neuron. Kybernetik 8:214–233

Chacron M, Pakdaman K, Longtin A (2003) Interspike interval correlations, memory, adaptation, and refractoriness in a leaky integrate-and-fire model with threshold fatigue. Neural Comput 15:253–278

Chance FS, Abbott LF, Reyes AD (2002) Gain modulation from balanced synaptic input. Neuron 35:773–782

Chhikara RS, Folks JL (1989) The Inverse Gaussian distribution: theory, methodology and applications. Marcel Dekker, New York

Cope DK, Tuckwell HC (1979) Firing rates of neurons with random excitation and inhibition. J Theor Biol 80:1–14

Cox DR (1962) Renewal theory. science paperbacks, Chapman and Hall, New York

Cox DR, Lewis PAW (1966) The statistical analysis of series of events. Methuen, London

Cox DR, Miller HD (1965) The theory of stochastic processes. Chapman and Hall, London

Cox DR, Smith WL (1954) On the Superposition of renewal processes. Biometrika 41:91–99

Destexhe A (1997) Conductance-based integrate-and-fire models. Neural Comput 9:503–514

Destexhe A, Paré D (1999) Impact of network activity on the integrative properties of neocortical neurons in vivo. J Neurophysiol 81: 1531–1547

Destexhe A, Rudolph M, Fellous J-M, Sejnowski TJ (2001) Fluctuating synaptic conductances recreate in-vivo-like activity in neocortical neurons. Neuroscirnce 107:13–24

Doiron B, Longtin A, Berman N, Maler L (2000) Subtractive and divisive inhibition: effect of voltage-dependent inhibitory conductances and noise. Neural Comput 13:227–248

Ermentrout GB (1996) Type I membranes, phase resetting curves, and synchrony. Neural Comput 8:979–1001

Ermentrout GB (1998) Linearization of F-I curves by adaptation. Neural Comput 10:1721–1729

Ermentrout GB, Kopell N (1986) Parabolic bursting in an excitable system coupled with a slow oscillation. SIAM J Appl Math 46:233–253

Feng J, Brown D (2000) Impact of correlated inputs on the output of the integrate-and-fire model. Neural Comput 12:671–692

Fourcaud N, Brunel N (2002) Dynamics of the firing probability of noisy integrate-and-fire neurons. Neural Comput 14:2057–2110

Fourcaud-Trocmé N, Brunel N (2005) Dynamics of the instantaneous firing rate in response to changes in input statistics. J Comput Neurosci 18:311–321

Fourcaud-Trocmé N, Hansel D, van Vreeswijk C, Brunel N (2003) How spike generation mechanisms determine the neuronal response to fluctuating inputs. J Neurosci 23:11628–11640

Fuhrmann G, Markram H, Tsodyks M (2002) Spike frequency adaptation and neocortical rhythms. J Neurophysiol 88:761–770

Fusi S, Mattia M (1999) Collective behavior of networks of linear (VLSI) integrate-and-fire neurons. Neural Comput 11:633–652

Geisler CD, Goldberg JM (1966) A stochastic model of the repetitive activity of neurons. Biophys J 6:53–69

Gerstein GL, Mandelbrot B (1964) Random walk models for the spike activity of a single neuron. Biophys J 4:41–68

Gerstner W (1995) Time structure of the activity in neural network models. Phys Rev E 51:738–758

Gerstner W (2001) A framework for spiking neuron models: the spike response model. In: Moss F, Gielen S (eds) The handbook of biological physics. Elsevier, Amsterdam, chap 12 pp 469–516

Gerstner W, Kistler WM (2002) Spiking neuron models: single neurons, populations, plasticity. Cambridge University Press Cambridge

Giugliano M, Darbon P, Arsiero M, Lüscher H-R, Streit J (2004) Single-neuron discharge properties and network activity in dissociated cultures of neocortex. J Neurophysiol 92:977–996

Gluss B (1967) A model for neuron firing with exponential decay of potential resulting in diffusion equations for probability density. Bull Math Biophysics 29:233–243

Gomez L, Budelli R, Saa R, Stiber M, Segundo JP (2005) Pooled spike trains of correlated presynaptic inputs as realizations of cluster point processes. Biol Cybern 92:110–127

Gutkin BS, Ermentrout GB (1998) Dynamics of membrane excitability determine interspike interval variability: a link between spike generation mechanisms and cortical spike train statistics. Neural Comput 10:1047–1065

Habib MK, Thavaneswaran A (1990) Inference for stochastic neuronal models. Appl Math Comput 38:51–73

Hansel D, van Vreeswijk C (2002) How noise contributes to contrast invariance of orientation tuning in cat visual cortex. J Neurosci 22:5118–5128

Hanson FB, Tuckwell HC (1983) Diffusion approximations for neuronal activity including synaptic reversal potentials. J Theor Neurobiol 2:127–153

Hill AV (1936) Excitation and accommodation in nerve. Proc R Soc B 119:305–355

Hodgkin AL, Huxley AF (1952) A quantitative description of membrane current and its application to conduction and excitation in nerve. J Physiol (London) 117:500–544

Hohn N, Burkitt AN (2001) Shot noise in the leaky integrate-and-fire neuron. Phys Rev E 63:031902

Holden AV (1976) Models of the stochastic theory of neurons. Springer, Berlin Heidelberg New York

Inoue J, Sate S, Ricciardi LM (1995) On the parameter extimation for diffusion models of single neuron's activities. Biol Cybern 73:209–221

Izhikevich EM (1999) Class 1 neural excitability, conventional synapses, weakly connected networks, and mathematical foundations of pulse-coupled models IEEE Trans Neural Netw 10:499–507

Izhikevich EM (2004) Which model to use for cortical spiking neurons? IEEE Trans Neural Netw 15:1063–1070

Jack JB, Noble D, Tsien RW (1985) Electric current flow in excitable cells. Clarendon, Oxford

Jackson BS (2004) Including long-range dependence in integrate-and-fire models of the high interspike-interval variability of cortical neurons. Neural Comput 16:2125–2195

Johannesma PIM (1968) Diffusion models for the stochastic activity of neurons. In: Caianiello ER (ed) Neural Networks. Springer, Berlin Heidelberg New York pp 116–144

Johnson DH (1996) Point process model of single-neuron discharges. J Comput Neurosci 3:275–299

Kallianpur G, Wolpert RL (1987) Weak convergence of stochastic neuronal models. In: Kimura M, Kallianpur G, Hida T (eds) Stochastic methods in biology. Springer, Berlin Heidelberg New York

Kempter R, Gerstner W, van Hemmen JL, Wagner H (1998) Extracting oscillations: neuronal coincidence detection with noisy periodic spike input. Neural Comput 10:1987–2017

Kistler WM, Gerstner W, van Hemmen JL (1997) Reduction of the Hodgkin–Huxley equations to a single-variable threshold model. Neural Comput 9:1015–1045

Knight BW (1972) Dynamics of encoding in a population of neurons. J Gen Physiol 59:734–766

Kohn AF (1989) Dendritic transformations on random synaptic inputs as measured from a neuron's spike trains – modeling and simulations. IEEE Trans Biomed Eng 36:44–54

Kryukov VI (1976) Wald's identity and random walk models for neuron firing. Adv Appl Probab 8:257–277

Kuhn A, Aertsen A, Rotter S (2003) Higher-order statistics of input ensembles and the response of simple model neurons. Neural Comput 15:67–101

Kuhn A, Aertsen A, Rotter S (2004) Neuronal integration of synaptic input in the fluctuation-driven regime. J Neurosci 24:2345–2356
La Camera G, Rauch A, Lüscher HR, Senn W, Fusi S (2004) Minimal models of adapted neuronal response to In vivo-like input currents. Neural Comput 16:2101–2124
Laing CR, Longtin A (2003) Dynamics of deterministic and stochastic paired excitatory-inhibitory delayed feedback. Neural Comput 15:2779–2822
Lamperti J (1966) Probability. Benjamin, New York
Lamperti J (1996) Probability 2nd edn. Wiley, New York
Lánská V, Lánský P (1998) Input parameters in a one-dimensional neuronal model with reversal potentials. BioSystems 48:123–129
Lánská V, Lánský P, Smith CE (1994) Synaptic transmission in a diffusion model for neural activity. J Theor Biol 166:393–406
Lánský P (1983) Inference for diffusion models of neuronal activity. Math Biosci 67:247–260
Lánský P (1984) On approximations of stein's neuronal model. J Theor Biol 107:631–647
Lánský P (1997) Sources of periodical force in noisy integrate-and-fire models of neuronal dynamics. Phys Rev E 55:2040–2043
Lánský P, Lánská V (1987) Diffusion approximation of the neuronal model with synaptic reversal potentials. Biol Cybern 56:19–26
Lánský P, Musila M (1991) Variable initial depolarization in stein's neuronal model with synaptic reversal potentials. Biol Cybern 64: 285–291
Lánský P, Radil T (1987) Stastical inference on spontaneous neuronal discharge patterns. Biol Cybern 55:299–311
Lánský P, Rodriguez R (1999a) The spatial properties of a model neuron increase its coding range. Biol Cybern 81:161–167
Lánský P, Rodriguez R (1999b) Two-compartment stochastic model of a neuron. Physica D 132:267–286
Lánský P, Rospars JP (1995) Ornstein–Uhlenbeck model neuron revisited. Biol Cybern 72:397–406
Lánský P, Sato S (1999) The stochastic diffusion models of nerve membrane depolarization and interspike interval generation. J Periph Nerv Syst 4:27–42
Lánský P, Smith CE (1989) The Effect of a random initial value in neural first-passage-time models. Math Biosci 93:191–215
Lánský P, Smith CE (1991) A one-dimensional neuronal diffusion model with reversal potentials. J Math Phys Sci 25:1–10
Lánský P, Sacerdote L, Tomassetti F (1995) On the comparison of Feller and Ornstein–Uhlenbeck models for neural activity. Biol Cybern 73:457–465
Lapicque L (1907) Recherches quantitatives sur l'excitation electrique des nerfs traitée comme une polarization. J Physiol Pathol Gen (Paris) 9:620–635
Latham PE, Richmond BJ, Nelson PG, Nirenberg S (2000) Intrinsic dynamics in neuronal networks. I. Theory. J Neurophysiol 83: 808–827
Lindner B (2004) Interspike interval statistics of neurons driven by colored noise. Phys Rev E 69:022901
Lindner B, Longtin A (2005a) Comment on: characterization of subthreshold voltage fluctuations in neuronal membranes by M Rudolph and A Destexhe. Neural Comput (in press)
Lindner B, Longtin A (2005b) Effect of an exponentially decaying threshold on the firing statistics of a stochastic integrate-and-fire neuron. J Theor Biol 232:505–521
Lindner B, Longtin A, Bulsara A (2003) Analytic expressions for rate and CV of a type I neuron driven by white Gaussian noise. Neural Comput 15:1761–1788
Liu Y-H, Wang X-J (2001) Spike-frequency adaptation of a generalized leaky integrate-and-fire model neuron. J Comput Neurosci 10:25–45
Longtin A, Doiron B, Bulsara AR (2002) Noise-induced divisive gain control in neuron models. BioSys 67:147–156
Mainen ZF, Sejnowski TJ (1995) Reliability of spike timing in neocortical neurons. Science 268:1503–1506
McCormick DA, Connors BW, Lighthall JW, Prince DA (1985) Cooperative electrophysiology of pyramidal and sparsely spiny stellate neurons of the neocortex. J Neurophysiol 54:782–805
Meffin H, Burkitt AN, Grayden DB (2004) An analytical model for the 'large, fluctuating conductance state' typical of neocortical neurons in vivo. J Comput Neurosci 16:159–175
Meffin H, Burkitt AN, Grayden DB (2005) Dynamically adjustable contrast enhancement from cortical background activity. Neurocomput 65-66:633–639
Middleton JW, Chacron MJ, Lindner B, Longtin A (2003) Firing statistics of a neuron model driven by long-range correlated noise. Phys Rev E 68:021920
Moreno R, de la Rocha J, Renart A, Parga N (2002) Response of spiking neurons to correlated inputs. Phys Rev Lett 89:288101
Moreno-Bote R, Parga N (2004) Role of synaptic filtering on the firing response of simple model neurons. Phys Rev Lett 92:028102
Murphy BK, Miller KD (2003) Multiplicative gain changes are induced by excitation or inhibition alone. J Neurosci 23:10040–10051
Musila M, Lánský P (1994) On the interspike intervals calculated from diffusion approximations of Stein's neuronal model with reversal potentials. J Theor Biol 171:225–232
Nilsson HG (1977) Estimation of parameters in a diffusion neuron model. Comput Biomed Res 10:191–197
Noble D, Stein RB (1966) The threshold conditions for initiation of action potentials by excitable cells. J Physiol 187:129–162
O'Neill WD, Lin JC, Ma Y-C (1986) Estimation and verification of a stochastic neuron model. IEEE Trans Biomed Eng 33:654–666
Paninski L, Pillow JW, Simoncelli EP (2004) Maximum likelihood extimation of a stochastic integrate-and-fire neural encoding model. Neural Comput 16:2533–2561
Papoulis A (1991) Probability, random variables, and stochastic processes, 3rd edn. McGraw-Hill, Singapore
Perkel DH, Gerstein GL, Moore GP (1967) Neuronal spike trains and stochastic point processes. I. The Single Spike Train. Biophys J 7:391–418
Plesser HE, Gerstner W (2000) Noise in integrate-and-fire neurons: from stochastic input to escape rates. Neural Comput 12:367–384
Plesser HE, Tanaka S (1997) Stochastic resonance in a model neuron with reset. Phys Lett A 225:228–234
Rauch A, La Camera G, Lüscher HR, Senn W, Fusi S (2003) Neocortical pyramidal cells respond as integrate-and-fire neurons to in vivo-like input currents. J Neurophysiol 90:1598–1612
Ricciardi LM (1976) Diffusion approximation for a multi-input model neuron. Biol Cybern 24:237–240
Ricciardi LM (1977) Diffusion processes and related topics in biology. Springer, Berlin Heidelberg New York
Ricciardi LM, Sacerdote L (1979) The Ornstein–Uhlenbeck process as a model for neuronal activity. Biol Cybern 35:1–9
Richardson MJE (2004) Effects of synaptic conductance on the voltage distribution and firing rate of spiking neurons. Phys Rev E 69:051918
Richardson MJE, Gerstner W (2005) Synaptic shot noise and conductance fluctuations affect the membrane voltage with equal significance. Neural Comput 17:923–947
Richardson MJE, Brunel N, Hakim V (2003) From subthreshold to firing-rate resonance. J Neurophysiol 89:2538–2554
Risken H (1996) The Fokker–Planck equation, 3rd edn. Springer, Berlin Heidelberg New York
Roy BK, Smith DR (1969) Analysis of the exponential decay model of the neuron showing frequency threshold effects. Bull Math Biophys 31:341–357
Rudd ME, Brown LG (1997) Noise Adaptation in integrate-and-fire neurons. Neural Comput 9:1047–1069
Rudolph M, Destexhe A (2003) The discharge variability of neocortical neurons during high-conductance states. Neurosci 119:855–873
Sakai Y, Funahashi S, Shinomoto S (1999) Temporally correlated inputs to leaky integrate-and-fire models can reproduce spiking statistics of cortical neurons. Neural Netw 12:1181–1190
Salinas E, Sejnowski TJ (2000) Impact of correlated synaptic input on output firing rate and variability in simple neuronal models. J Neurosci 20:6193–6209
Salinas E, Sejnowski TJ (2002) Integrate-and-fire neurons driven by correlated stochastic input. Neural Comput 14:2111–2155

Salinas E, Thier P (2000) Gain modulation: a major computational principle of the central nervous system. Neuron 27:15–21
Schrödinger E (1915) Zur Theorie der Fall- und Steigversuche an Teilchen mit Brownscher Bewegung. Phys Zeitschr 16:289–295
Shadlen MN, Newsome WT (1994) Noise, neural codes and cortical organization. Curr Opin Neurobiol 4:569–579
Shadlen MN, Newsome WT (1998) The variable discharge of cortical neurons: implications for connectivity, computation, and information coding. J Neurosci 18:3870–3896
Siebert WM (1969) On stochastic neural models of the diffusion type. Prog Rep 94:281–287, Res Lab Electronics, MIT, Cambridge
Siegert AJF (1951) On the first passage time probability problem. Phys Rev 81:617–623
Smith CE, Smith MV (1984) Moments of voltage trajectories for Stein's model with synaptic reversal potentials. J Theor Neurobiol 3:67–77
Softky WR, Koch C (1992) Cortical cells should fire regularly, but do not. Neural Comput 4:643–646
Softky WR, Koch C (1993) The highly irregular firing of cortical cells is inconsistent with temporal integration of random EPSPs. J Neurosci 13:334–350
Stein RB (1965) A theoretical analysis of neuronal variability. Biophys J 5:173–194
Stein RB (1967) Some models of neuronal variability. Biophys J 7: 37–68
Stevens CF, Zador AM (1998) Input synchrony and the irregular firing of cortical neurons. Nature Neurosci 1:210–217
Stirzaker D (2005) Stochastic processes and models. Oxford University Press, New York
Stroeve S, Gielen S (2001) Correlation between uncoupled conductance-based integrate-and-fire neurons due to common and synchronous presynaptic firing. Neural Comput 13:2005–2029
Sugiyama H, Moore GP, Perkel DH (1970) Solutions for a stochastic model of neuronal spike production. Math Biosci 8:323–341
Svirskis G, Rinzel J (2000) Influence of temporal correlation of synaptic input on the rate and variability of firing in neurons. Biophys J 79:629–637
Tabak J, Murphey CR, Moore LE (2000) Parameter estimation methods for single neuron models. J Comput Neurosci 9:215–236
Tiesinga PHE, José JV, Sejnowski TJ (2000) Comparison of current-driven and conductance-driven neocortical model neurons with Hodgkin–Huxley voltage-gated channels. Phys Rev E 62:8413–8419
Troyer TW, Miller KD (1997) Physiological gain leads to high ISI variability in a simple model of a cortical regular spiking cell. Neural Comput 9:971–983
Tuckwell HC (1977) On stochastic models of the activity of single neurons. J Theor Biol 65:783–785
Tuckwell HC (1978a) Neuronal interspike time histograms for a random input model. Biophys J 21:289–290
Tuckwell HC (1978b) Recurrent inhibition and afterhyperpolarization: effects on neuronal discharge. Biol Cybern 30:115–123
Tuckwell HC (1979) Synaptic transmission in a model for stochastic neural activity. J Theor Biol 77:65–81
Tuckwell HC (1988a) Introduction to Theoretical Neurobiology. In: linear cable theory and dendritic structure, vol 1. Cambridge University Press, Cambridge
Tuckwell HC (1988b) Introduction to Theoretical Neurobiology. In: Nonlinear and stochastic theories, vol 2. Cambridge University Press, Cambridge
Tuckwell HC, Cope DK (1980) Accuracy of neuronal interspike times calculated from a diffusion approximation. J Theor Biol 83:377–387
Tuckwell HC, Richter W (1978) Neuronal interspike time distributions and the estimation of neurophysiological and neuroanatomical paramaters. J Theor Biol 71:167–183
Tuckwell HC, Wan FYM (1984) First passage time of Markov processes to moving barriers. J Appl Probab 21:695
Uhlenbeck GE, Ornstein LS (1930) On the theory of Brownian motion. Phys Rev 36:823–841
Usher M, Stemmler M, Koch C, Olami Z (1994) Network amplification of local fluctuations causes high spike rate variability, fractal firing patterns and oscillatory local field potentials. Neural Comput 6:795–836
van Kampen NG (1992) Stochastic processes in physics and chemistry. North-Holland, Amsterdam
Wang X-J (1998) Calcium Coding and adaptive temporal computation in cortical pyramidal neurons. J Neurophysiol 79:1549–1566
Wehmeier U, Dong D, Koch C, Van Essen D (1989) Modeling the mammalian visual system. In: Koch C, Segev I (eds) Methods in neuronal modeling: from synapses to networks, Chap 10. MIT, Cambridge pp 335–360
Wilbur WJ, Rinzel J (1982) An Analysis of Stein's model for stochastic neuronal excitation. Biol Cybern 45:107–114
Wilbur WJ, Rinzel J (1983) A theoretical basis for large coefficient of variation and bimodality in neuronal interspike interval distributions. J Theor Biol 105:345–368
Yu Y, Lee TS (2003) Dynamical mechanisms underlying contrast gain control in single neurons. Phys Rev E 68:011901